UNIVERSITATEA BABEŞ–BOLYAI
Facultatea de Chimie şi Inginerie Chimică

UNIVERSITÄT LEIPZIG
Fakultät für Chemie und Mineralogie

Summary of the Ph. D. Thesis

Synthesis and Reactivity of Heterotopic Ligands Containing As/P, As/S/P and As/S/As as Donor Atoms

Scientific advisors

Prof. Dr. Luminiţa Silaghi-Dumitrescu
Prof. Dr. Evamarie Hey-Hawkins

Ph.D. student

Imola Bartók (căs. Sárosi)

Cluj-Napoca
–2012–

JURY

PRESIDENT

Conf. Dr. Cornelia MAJDIK

REVIEWERS

CSI Dr. Otilia COSTIŞOR - Institutul de Chimie Timişoara al Academiei Române, Timişoara.

Prof. Dr. Simona Luminiţa OPREAN - Universitatea de Medicină şi Farmacie Iuliu Haţieganu, Cluj-Napoca.

Acad. Prof. Dr. Ionel HAIDUC - Facultatea de Chimie şi Inginerie Chimică, Universitatea Babeş-Bolyai, Cluj-Napoca, President of the Romanian Academy.

Date of public defense: February 27, 2012

CONTENTS (as in the full text)

Keywords: heteropolytopic S,P,As-ligands; transition metal complexes; structural isomerism; DFT calculations; molecular structures.

Introduction

1. Literature overview

There is a considerable current interest in heterodonor polydentate ligands involving tertiary phosphine and arsine groups in combinations with nitrogen, oxygen or sulfur donors. Ligands incorporating both thiolate and tertiary phosphine or arsine donor atoms are especially interesting, as their combination is likely to confer unusual structures and reactivities on their metal complexes.

Tertiary phosphine and arsine ligands derived from thiophenol have been shown to be very versatile ligands that form stable complexes with a wide range of transition metals. The low ionisation energy of sulfur and the presence of several lone pairs of electrons (three in the case of a thiolate anion) offer the possibility of a rich sulfur-based chemistry of the complexes. Metal thiolates can form complexes with various nuclearities and great structural complexity as a result of the tendency of the thiolato ligands to bridge metal centres.[5]

Further on, the literature overview focuses on three major groups of thiophenol-based heterotopic E,S ligands (E = As, P):

1) phenylthio(diphenyl)phosphine and -arsine ligands: $EPh_2(SPh)$
2) bidentate phosphanyl- and arsanylarylthiol ligands: 1-EPh_2-2-SH-C_6H_4
3) tridentate thiophenol ligands bearing two tertiary P donor groups: 2,6-$(Ph_2PCH_2)_2C_6H_3SH$ and 2,6-$(Ph_2P)_2C_6H_3SH$.

The next three subchapters describe the coordination chemistry of these ligands with transition metal complexes; the metal-mediated cleavage of the E–S bond in the $EPh_2(SPh)$ ligands, respectively the coordination of the mixed-donor E,S chelating groups of the bi- and tridentate ligands is being investigated.

Original contributions

2. Aims of this work

Based on the literature overview, one can see that the coordination chemistry of thiophenol-based heterodonor P,S and As,S ligands has been explored to some extent, but examples of ligands incorporating all three donor atoms are still unknown. Thus, the design of some P,As,S-tridentate ligands seems reasonable, since all three atoms are excellent donors for a wide range of metals. Therefore, the synthesis and structural characterisation of the following novel heterotopic P,As,S ligands and the investigation of their coordination chemistry with transition metal complexes was proposed.

The designed thiophenol-based novel heterotopic P,As,S ligands can be divided in two categories:

1. The ligands 1-PPh_2-2-S($AsPh_2$)C_6H_4 (**1**) and 1-$AsPh_2$-2-S(PPh_2)C_6H_4 (**2**) incorporate an E–S bond and have an EPh_2 group (E = As, P) in the *ortho*-position to sulfur. Thus, these ligands combine the properties of phenylthio(diphenyl)phosphine/-arsine and phosphanyl-/arsanylbenzenethiol. However, these ligands should also exhibit a wide range of possible bonding modes and would allow to study the effect of the EPh_2 group in *ortho* position on cleavage of the E–S bond. Furthermore, **1** and **2** could act as potentially tridentate ligands for a wide range of metals (Scheme 15).

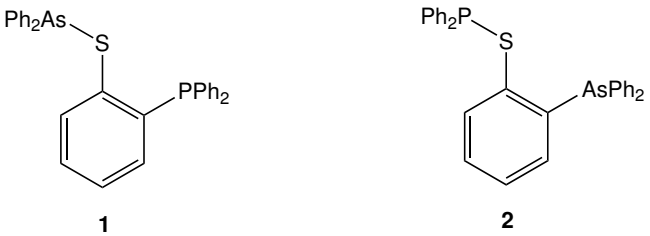

1 **2**

Scheme 15. 1-PPh_2-2-S($AsPh_2$)C_6H_4 (**1**), 1-$AsPh_2$-2-S(PPh_2)C_6H_4 (**2**).

2. Thiophenolate ligands with two flanking tertiary E donor groups in the *ortho*-positions (E = As, P) can capture and bring two metal atoms close to each other by forming heteroatom-bridged bimetallic complexes. By introducing slightly different donor atoms in the *ortho*-positions, the coordination preferences of different metals could also be investigated. The proposed ligands are shown on Scheme 17.

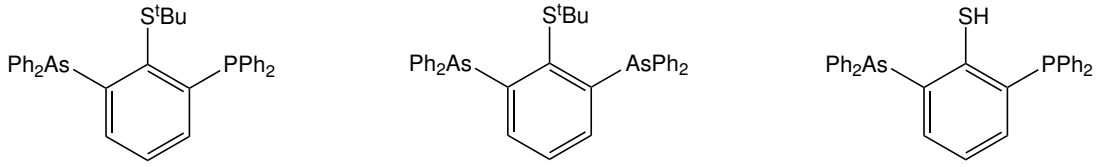

3, **SPAs** **4**, **SAs2** **5**, **SHPAs**

Scheme 17. 1-PPh_2-2-S(C_4H_9)-3-$AsPh_2$-C_6H_3 (**3**, **SPAs**), 1,3-$AsPh_2$-2-S(C_4H_9)C_6H_3 (**4**, **SAs2**), 1-PPh_2-2-SH-3-$AsPh_2$-C_6H_3 (**5**, **SHPAs**).

3. Heterotopic ligands containing As/P, As/S/P and As/S/As as donor atoms

3.1. Heterotopic ligands containing As/P as donor atoms

3.1.1 Synthesis of 1-PPh_2-2-S($AsPh_2$)C_6H_4 (**1**) and 1-$AsPh_2$-2-S(PPh_2)C_6H_4 (**2**)

The synthesis of these compounds requires the preparation of the starting materials which are commercially not available; Ph_2AsCl,[64,65] 1-PPh_2-2-SH-C_6H_4 (PSH)[34,38] and 1-$AsPh_2$-2-SH-C_6H_4 (AsSH)[35] were prepared according to literature procedures.

Treatment of a stirred toluene solution of PSH or AsSH with *n*-butyllithium at 0 °C resulted in a pale yellow suspension. After 20 h at room temperature the slurry of the mono-lithiated product was treated with the appropriate electrophile to give the desired compounds **1** and **2** as pale yellow solids (Scheme 19).

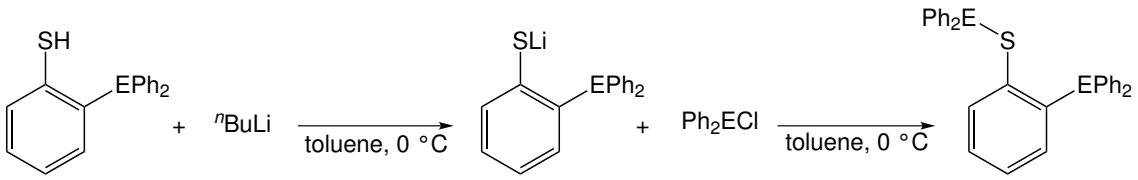

Scheme 19. Synthetic route towards 1-PPh_2-2-S($AsPh_2$)C_6H_4 (**1**) and 1-$AsPh_2$-2-S(PPh_2)C_6H_4 (**2**).

The compounds show signals in the ^{1}H NMR spectra in the range of δ = 7.4–6.7 due to the aromatic protons and each of them exhibits a singlet in the $^{31}P\{^1H\}$ NMR spectra: δ = –12.5 (**1**) and δ = 37.5 (**2**). In the EI mass spectra of **1** and **2** the corresponding molecular ion peaks as well as appropriate fragmentations were observed.

3.1.2 Molecular structure of 1-PPh_2-2-S($AsPh_2$)C_6H_4 (**1**)

Compound **1** crystallises in the monoclinic space group $P2_1/c$ with two independent molecules in the asymmetric unit. The molecular structure is shown in Figure 12. The phosphorus and arsenic atoms are coordinated in a slightly distorted trigonal-pyramidal fashion (Table 1).

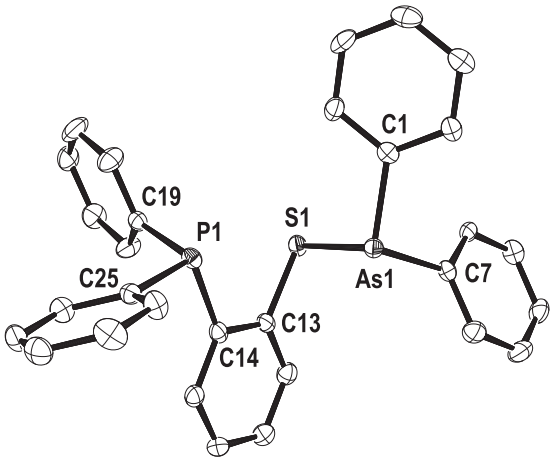

Figure 12. Molecular structure of 1-PPh_2-2-S($AsPh_2$)C_6H_4 (**1**). Hydrogen atoms are omitted for clarity.

Table 1. Selected bond lengths and angles for **1**.

Bond lengths [pm]		Bond angles [°]	
As(1)–S(1)	226.6(1)	C(1)–As(1)–C(7)	100.7(2)
S(1)–C(13)	178.4(4)	C(1)–As(1)–S(1)	99.2(1)
P(1)–C(19)	183.7(4)	C(7)–As(1)–S(1)	98.3(1)
P(1)–C(14)	183.8(4)	C(13)–S(1)–As(1)	94.4(1)
P(1)–C(25)	184.3(4)	C(19)–P(1)–C(14)	102.2(1)
		C(19)–P(1)–C(25)	103.2(2)
		C(14)–P(1)–C(25)	100.7(2)

3.1.3 Theoretical calculations for 1-PPh_2-2-$S(AsPh_2)C_6H_4$ (**1**)

Figure 12 shows the highest occupied molecular orbital (HOMO) of **1**, which is predominantly made of the phosphorus and sulfur lone pairs. This specific nature of the HOMO makes the P,S chelating pocket of **1** most suitable for an electrophilic attack. The lowest unoccupied molecular orbital (LUMO) of **1** is predominantly an As–S antibonding orbital (Figure 14). Not surprisingly, the P–C(14) homolytic bond dissociation energy is significantly higher than the energy required to cleave the As–S bond (Table 2).

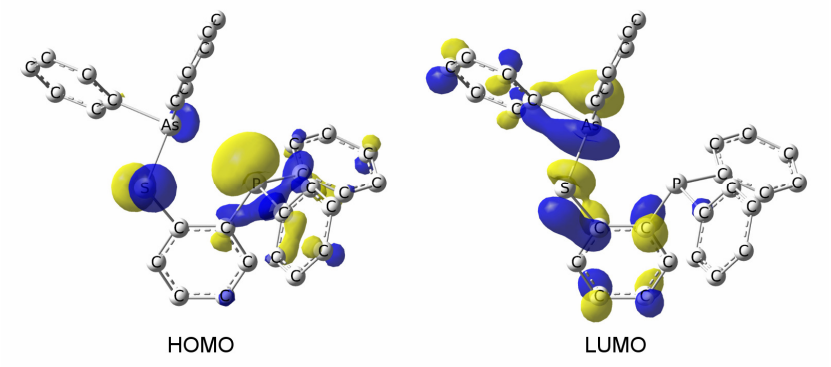

Figure 14. HOMO and LUMO of **1**.

Table 2. Bond dissociation energies for 1-PPh_2-2-S($AsPh_2$)C_6H_4 (**1**), reported in kJ mol^{-1}.

Process	$\Delta G°_{(gas)}$	$\Delta G°_{(toluene)}$
1a: **1** → $[AsPh_2]^{\bullet}$ + $[1\text{-}PPh_2\text{-}2\text{-}SC_6H_4]^{\bullet}$	172.5	169.2
1b: **1** → $[AsPh_2]^{-}$ + $[1\text{-}PPh_2\text{-}2\text{-}SC_6H_4]^{+}$	579.5	390.6
1c: **1** → $[AsPh_2]^{+}$ + $[1\text{-}PPh_2\text{-}2\text{-}SC_6H_4]^{-}$	595.0	399.0
2a: **1** → $[PPh_2]^{\bullet}$ + $[S(AsPh_2)C_6H_4]^{\bullet}$	227.5	226.3
2b: **1** → $[PPh_2]^{-}$ + $[S(AsPh_2)C_6H_4]^{+}$	575.8	390.5
2c: **1** → $[PPh_2]^{+}$ + $[S(AsPh_2)C_6H_4]^{-}$	568.8	369.9

3.2. Heterotopic ligands containing As/S/P and As/S/As as donor atoms

3.2.1 Synthesis of 1-PPh_2-2-S(C_4H_9)-3-$AsPh_2$-C_6H_3 (**3**, **SPAs**), 1,3-$AsPh_2$-2-S(C_4H_9)C_6H_3 (**4**, **SAs2**) and 1-PPh_2-2-SH-3-$AsPh_2$-C_6H_3 (**5**, **SHPAs**)

By treatment of 1-PPh_2-2-S(C_4H_9)C_6H_4 with ^{n}BuLi in the presence of TMEDA and with Ph_2AsCl, **SPAs** could be synthesised in moderate yields. Scheme 20 shows the involved reaction steps.

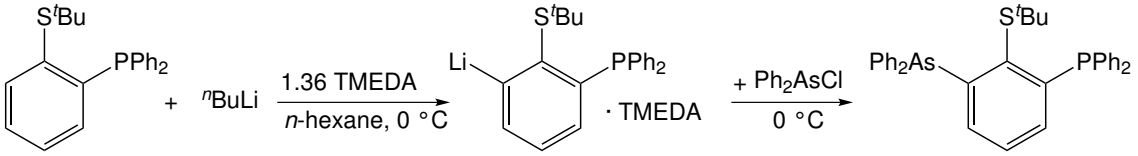

Scheme 20. Synthetic route towards **SPAs** (**3**).

The synthesis of **SAs2** required the preparation of 1-$AsPh_2$-2-S(C_4H_9)C_6H_4 (**4a**). TMEDA was added to a solution of *tert*-butyl phenyl sulfide and *n*-butyllithium in *n*-hexane.[83] A white precipitate has formed and the dropwise addition of Ph_2AsCl was carried out *in situ* with this suspension (Scheme 21). After workup, **4a** was obtained as a white solid in good yield.

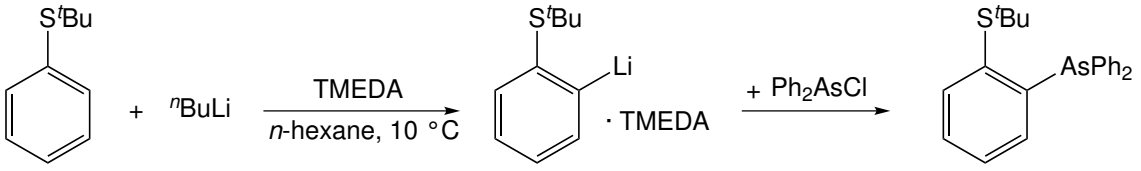

Scheme 21. Synthesis of 1-AsPh$_2$-2-S(C$_4$H$_9$)C$_6$H$_4$ (**4a**).

4a was monolithiated and the second arsenic group was introduced into the second *ortho*-position. The reaction steps involved are very similar to that of **SPAs** (Scheme 22). **SAs2** was obtained in moderate yield as a pale yellow solid.

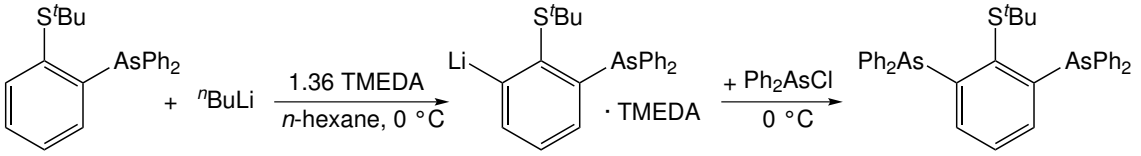

Scheme 22. Synthetic route towards **SPAs** (**4**).

In order to restore the –SH function, **SPAs** was reacted with lithium naphthalenide, followed by acidification of the reaction media (Scheme 23). After workup **SHPAs** was isolated as a waxy pale yellow solid in good yield.

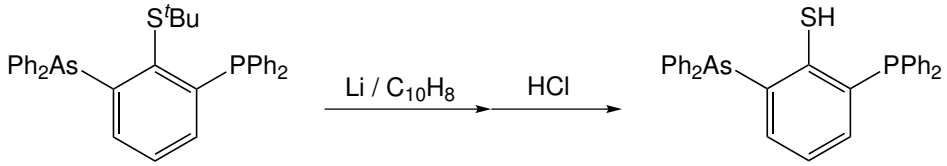

Scheme 23. Synthesis of **SHPAs** (**5**).

Compounds **3**–**5** show signals in the ^{1}H NMR spectra in the range of δ = 7.4–6.7 due to the aromatic protons, a singlet is visible at δ = 1.65 (**SPAs**), δ = 1.35 (**4a**) and δ = 1.65 (**SAs2**) assigned to the ^{t}Bu protons and a doublet at δ = 4.75 ($^4J_{PH}$ = 4.5 Hz) (**SHPAs**) for the SH proton. **SPAs** exhibits a singlet in the ^{31}P{^{1}H} NMR spectra at δ = –6.7, while the replacement of the ^{t}Bu group with a hydrogen atom results in a high-field shift, **SHPAs** showing a singlet at δ = –11.7. In the ESI and EI mass spectra of **3**–**5**

the corresponding molecular ion peaks as well as appropriate fragmentations were observed.

3.2.2 Molecular structures of **4a**, **SPAs**, **SAs2** and **SHPAs**

4a crystallises in the monoclinic space group $P2_1/c$ with eight molecules in the unit cell and two molecules in the asymmetric unit. The molecular structure of **4a** is depicted in Figure 16. Compound **4a** adopts a conformation where the $AsPh_2$ and *tert*-butylthio substituents are rotated around the bonds connecting the heteroatoms to the central phenyl ring to minimise steric interactions between the ^{t}Bu group and the phenyl rings. The arsenic atom is coordinated in a slightly distorted pyramidal fashion by the three carbon atoms of the aromatic rings (Table 3), the angles being close to the tetrahedral angle of 109.5°.

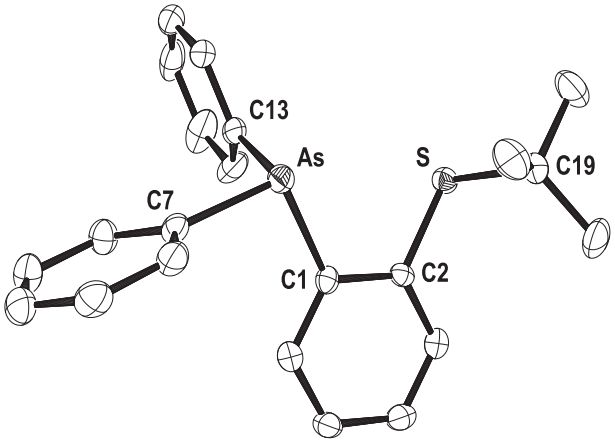

Figure 16. Molecular structure of 1-$AsPh_2$-2-S(C_4H_9)C_6H_4 (**4a**). Hydrogen atoms are omitted for clarity.

Table 3. Selected bond lengths and angles for (**4a**).

Bond lengths [pm]		Bond angles [°]	
C(2)–S(1)	178.2(2)	C(13)–As(1)–C(7)	97.8(1)
S(1)–C(19)	185.0(3)	C(13)–As(1)–C(1)	101.0(1)
As(1)–C(13)	195.2(3)	C(7)–As(1)–C(1)	97.9(1)
As(1)–C(7)	196.3(3)	C(2)–S(1)–C(19)	105.5(1)
As(1)–C(1)	196.6(2)		

SPAs, **SAs2** and **SHPAs** crystallise in the triclinic space group $P\bar{1}$ with two molecules in the unit cell. The molecular structures of **SPAs** and **SAs2** are isotypical (Figure 17), both molecules adopt a conformation where the PPh_2/$AsPh_2$ and *tert*-butylthio substituents are rotated around the bonds connecting the heteroatoms to the central phenyl ring to minimise the steric interactions between the ^{t}Bu group and the phenyl rings.

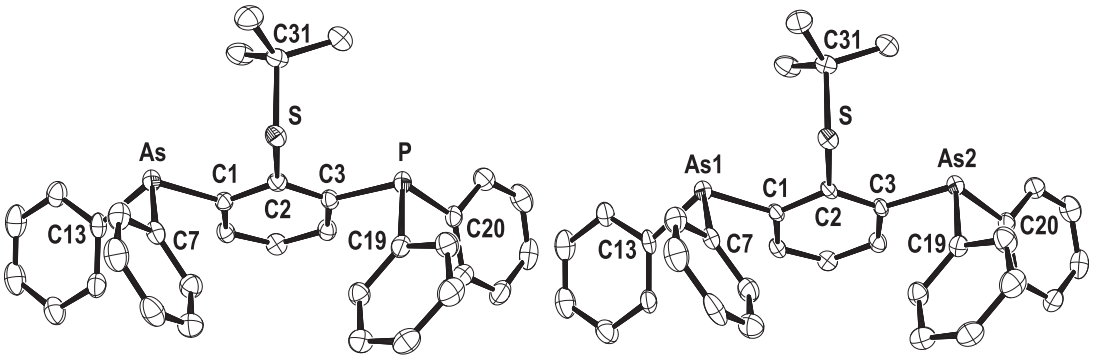

Figure 17. Molecular structure of **SPAs** (**3**) and **SAs2** (**4**). Hydrogen atoms are omitted for clarity.

Due to the restored –SH function in the molecular structure of **SHPAs**, the PPh_2 and $AsPh_2$ substituents are no longer forced to only one side of the plane of the central phenyl ring. In all three structures the phosphorus and arsenic atoms are coordinated in a slightly distorted pyramidal fashion by the three carbon atoms of the aromatic rings, the bond angles being close to the tetrahedral angle of 109.5°. All bond distances and angles are in the expected range (Table 4) and comparable to other phosphanylarylthiols[36] and to precursor **4a**.

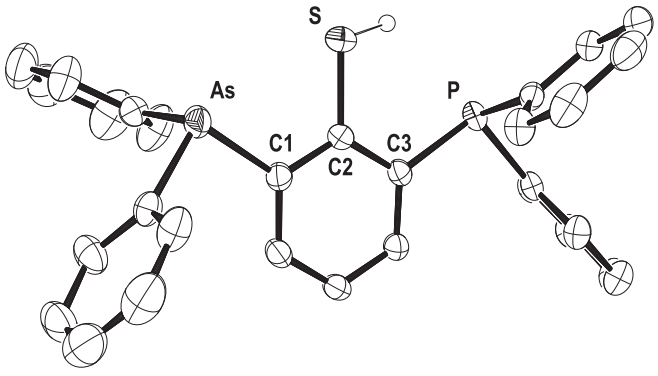

Figure 18. Molecular structure of **SHPAs** (**5**). Aryl hydrogen atoms are omitted for clarity.

Table 4. Selected bond lengths and angles for **SPAs** (**3**), **SAs2** (**4**) and **SHPAs** (**5**).

Bond lengths [pm] and angles [°]	**SPAs** (**3**)	**SAs2** (**4**)	**SHPAs** (**5**)
As(1)–C(7)	191.2(2)	195.8(3)	192.2(2)
As(1)–C(13)	192.3(2)	197.2(3)	190.7(2)
As(1)–C(1)	192.4(2)	196.3(3)	194.1(2)
P(As2)–C(19)	190.4(2)	195.8(3)	189.6(2)
P(As2)–C(25)	190.5(2)	195.6(3)	189.3(2)
P(As2)–C(3)	192.3(2)	197.0(2)	190.2(2)
S(1)–C(2)	178.6(2)	178.7(3)	177.3(2)
S(1)–C(31)	187.3(2)	187.1(3)	
S(1)–H(1S)	–	–	130.7(2)
S(1)–H(1SF)	–	–	134.0(2)
C(7)–As(1)–C(13)	98.2(9)	98.1(1)	100.2(9)
C(7)–As(1)–C(1)	98.7(8)	98.6(1)	97.4(8)
C(13)–As(1)–C(1)	101.2(8)	101.0(1)	100.3(8)
C(19)–P(As2)–C(25)	98.5(9)	98.3(1)	98.8(8)
C(19)–P(As2)–C(3)	97.6(9)	97.9(1)	101.0(8)
C(25)–P(As2)–C(3)	100.1(8)	100.1(1)	99.5(8)
C(2)–S(1)–C(31)	105.0(9)	105.2(1)	
C(2)–S(1)–H(1S)			102.0(2)
C(2)–S(1)–H(1SF)			98.0(5)

3.2.3 Theoretical calculations for **SPAs** (**3**) and **SHPAs** (**5**)

The HOMO of **SPAs** is mainly made of the lone pairs on sulfur, phosphorus and arsenic, with the maximum atomic orbital coefficient at sulfur (0.27) followed by 0.18 on phosphorus and 0.11 at arsenic (Figure 19). This indicates that the P,S chelating pocket might be favoured over the As,S unit during an electrophilic attack. The LUMO of **SPAs** is mainly made of unoccupied orbitals on the carbon atoms of the central aromatic ring, but also shows a slight S–C(^{t}Bu) antibonding character (Figure 19).

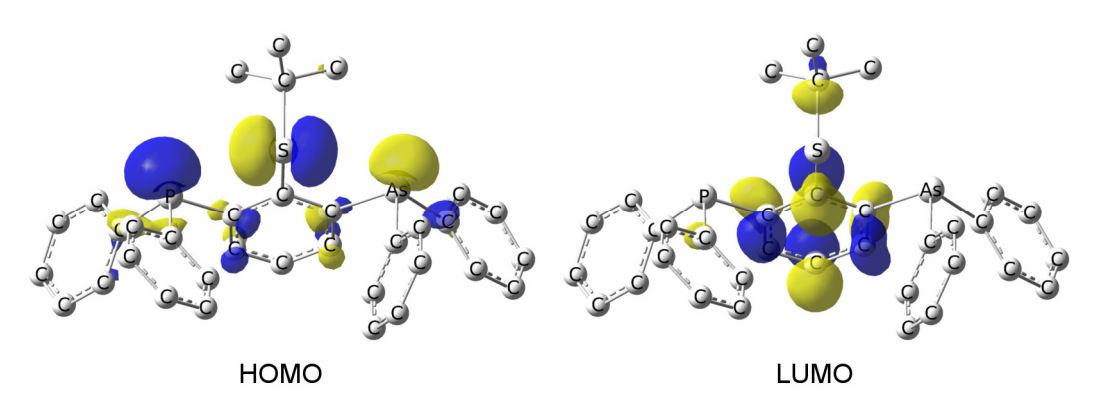

Figure 19. HOMO and LUMO of **SPAs**.

Removing the ^{t}Bu group from **SPAs** results in the HOMO to be localised at the P,S chelating pocket only. Thus, the HOMO of **SHPAs** is mainly made of the lone pairs on sulfur and phosphorus, with the maximum atomic orbital coefficient at sulfur (0.24) followed by 0.21 on phosphorus (Figure 21).

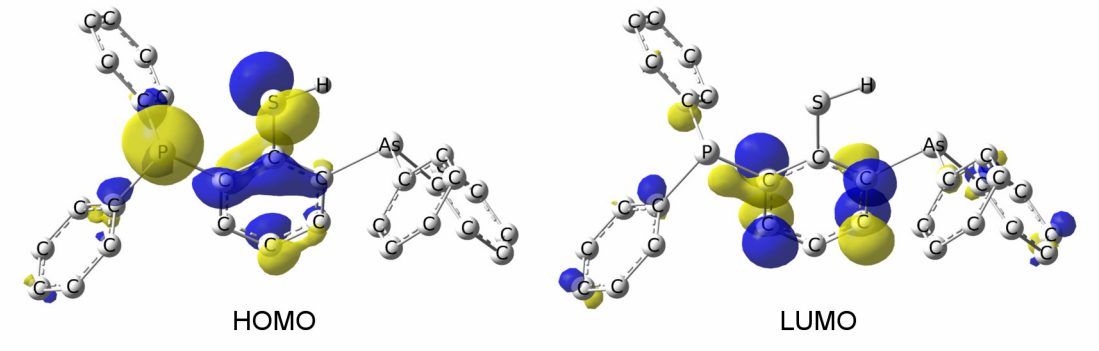

Figure 21. HOMO and LUMO of **SHPAs**.

Furthermore, the gas phase As–C(1) and P–C(3) bond dissociation energies for both homolytic and heterolytic bond cleavage were also calculated for **SPAs** (see Figure 17 for atom numbering). In both cases the homolytic bond dissociation energies are significantly smaller than the energies required for a heterolytic bond cleavage of either type (Table 5). The homolytic As–C(1) bond dissociation energy (1a) is somewhat higher than the energy required for cleaving the P–C(3) bond (2a). Thus, the As–C(1) bond seems to be stronger than the P–C(3) bond.

Table 5. Bond dissociation energies for **SPAs** (**3**), reported in kJ mol^{-1}.

Process	$\Delta G°_{(gas)}$	$\Delta G°_{(n\text{-hexane})}$
1a: **SPAs (3)** → $[AsPh_2]^{\bullet}$ + $[1\text{-}PPh_2\text{-}2\text{-}S(C_4H_9)\text{-}C_6H_3]^{\bullet}$	239.0	240.7
1b: **SPAs (3)** → $[AsPh_2]^{-}$ + $[1\text{-}PPh_2\text{-}2\text{-}S(C_4H_9)\text{-}C_6H_3]^{+}$	587.0	439.0
1c: **SPAs (3)** → $[AsPh_2]^{+}$ + $[1\text{-}PPh_2\text{-}2\text{-}S(C_4H_9)\text{-}C_6H_3]^{-}$	763.2	617.3
2a: **SPAs (3)** → $[PPh_2]^{\bullet}$ + $[1\text{-}AsPh_2\text{-}S(C_4H_9)\text{-}C_6H_3]^{\bullet}$	209.8	212.1
2b: **SPAs (3)** → $[PPh_2]^{-}$ + $[1\text{-}AsPh_2\text{-}S(C_4H_9)\text{-}C_6H_3]^{+}$	738.6	592.6
2c: **SPAs (3)** → $[PPh_2]^{+}$ + $[1\text{-}AsPh_2\text{-}S(C_4H_9)\text{-}C_6H_3]^{-}$	736.5	585.3

4. Coordination chemistry of 1-PPh_2-2-$S(AsPh_2)C_6H_4$ (1) with transition metal complexes

4.1. Coordination chemistry of 1 with group 10 metal(II) complexes

4.1.1 Synthesis and spectroscopic properties of Ni (**6**), Pd (**7**, **8**) and Pt (**9**, **10**) complexes

The nickel(II) (**6**), palladium(II) (**7**, **8**) and platinum(II) (**9**, **10**) complexes were synthesised by reaction of compound **1** with $[NiCl_2{\cdot}6H_2O]$, $[PdCl_2(cod)]$ and $[PtI_2(cod)]$ (cod = 1,5-cyclooctadiene), respectively.[85] Cleavage of the As–S bond of **1** and coordination of the resulting phosphanylthiolato ligand $(SC_6H_4\text{-}2\text{-}PPh_2)^{-}$ (SC_6H_4-2-PPh_2 = P,S) was observed in each case.

The 1:1 reaction of **1** and $NiCl_2{\cdot}6\ H_2O$ in THF at room temperature resulted in the formation of the known bischelate complex *trans*-$[Ni\{(SC_6H_4\text{-}2\text{-}PPh_2)\text{-}\kappa^2S,P\}_2]$ (**6**)[54,55]. The $^{31}P\{^1H\}$ NMR spectra of the reaction mixture show compound **6** as the only phosphorus-containing reaction product, even after prolonged standing in solution. Palladium(II) and platinum(II) complexes **7**–**10** were synthesised by reaction of **1** with $[MX_2(cod)]$ (M = Pd, X = Cl; M = Pt, X = I) in a 1:1 ratio. Shorter reaction times (4 h, M = Pd; 1 week, M = Pt) gave the trinuclear complexes [(*cis*-M{(μ-*S*-SC_6H_4-2-PPh_2)-

$\kappa^2S,P\}_2$)-MX_2-MX{(μ-*S*-SC_6H_4-2-PPh_2)-$\kappa^2S,P\}$] [M = Pd, X = Cl (**8**); M = Pt, X = I (**10**)], while the trimeric trinuclear isomers [MX{(μ-*S*-SC_6H_4-2-PPh_2)-$\kappa^2S,P\}]_3$ [M = Pd, X = Cl (**7**); M = Pt, X = I (**9**)] were obtained after reaction times of two weeks. The isolated trinuclear isomeric products **7** and **9** or **8** and **10**, respectively, contain only the P,S-coordinating phosphanylarylthiolato ligand. The eliminated $AsPh_2$ group was observed in the filtrate after isolation of **7**–**10** by ESI mass spectrometry, which showed different oxidised species of dimerised $AsPh_2$. The possible steps involved in the formation of complexes **7**–**10** are depicted on Scheme 25.

Since the $AsPh_2$ group is eliminated and does not participate in coordination to the metal centre, the reaction of HSC_6H_4-2-PPh_2 with [$PdCl_2$(cod)] and [PtI_2(cod)] was reinvestigated. The 2:1 or 1:1 reactions conducted in the presence of NEt_3 always led to the formation of *cis* and *trans* bischelates. When the deprotonating agent was excluded from the reaction mixture, exclusive formation of the trinuclear complex was preferred in the reaction with [$PdCl_2$(cod)], while the reaction with [PtI_2(cod)] led to *cis*- and *trans*-[$M(P,S)_2$] complexes as main reaction products and traces of trimeric complex **7**.

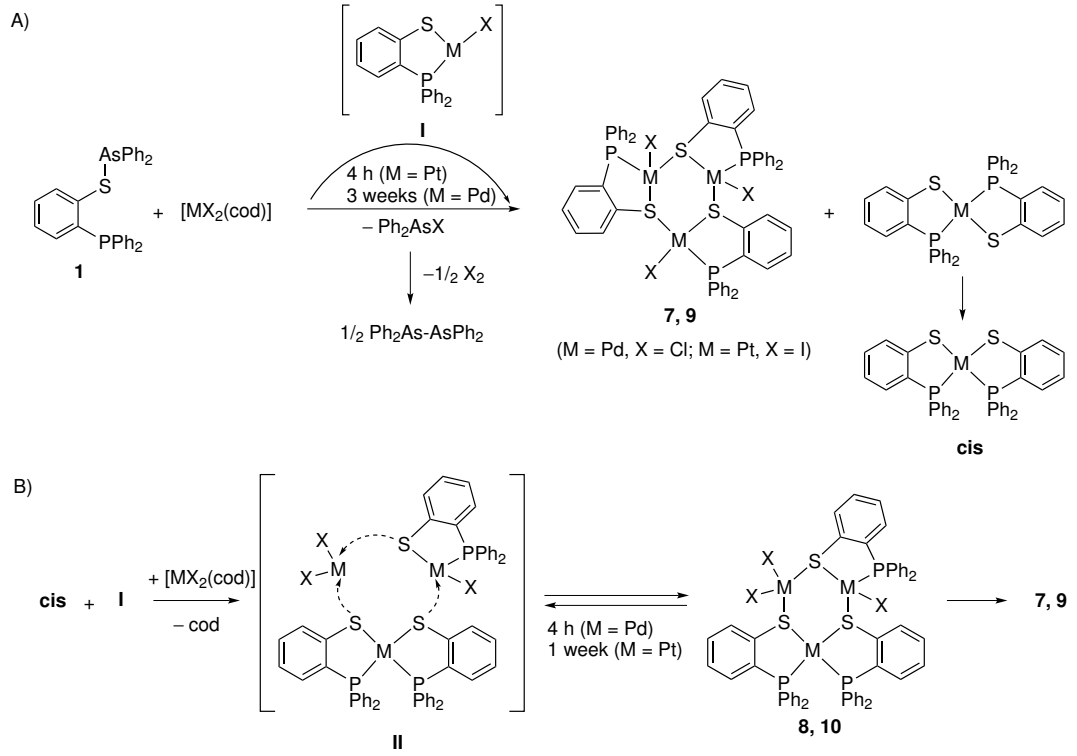

Scheme 25. Possible steps involved in the formation of complexes **7**–**10**.

4.1.2 Molecular structures of Pd (**7**, **8**) and Pt (**9**, **10**) complexes

Complexes **7**–**9** crystallise in the monoclinic space group $P2_1/c$ and compound **10** in $P2_1/n$ with four molecules in the unit cell. They consist of a six-membered M_3S_3 ring (M = Pd, Pt) in which the S atoms of the phosphanylthiolato ligand act as bridges between two metal atoms. In the case of the symmetric trimeric complexes **7** and **9** (Figure 25), additionally each P atom binds to one metal centre resulting in MSC_2P rings. Every metal atom is thus coordinated by two S, one P, and one terminally bonded X atom [X = Cl (**7**), I (**9**)] in a distorted square-planar fashion with the two sulfur atoms in a *cis* arrangement.

Complexes **8** and **10** (Figure 26) are built up of three subunits: a *cis* bischelate $M(P,S)_2$ is connected through the S atoms to an MX(P,S) and an MX_2 unit to form the M_3S_3 ring. The intramolecular M···M distances are all greater than 356 pm, indicating no metal–metal bonding.

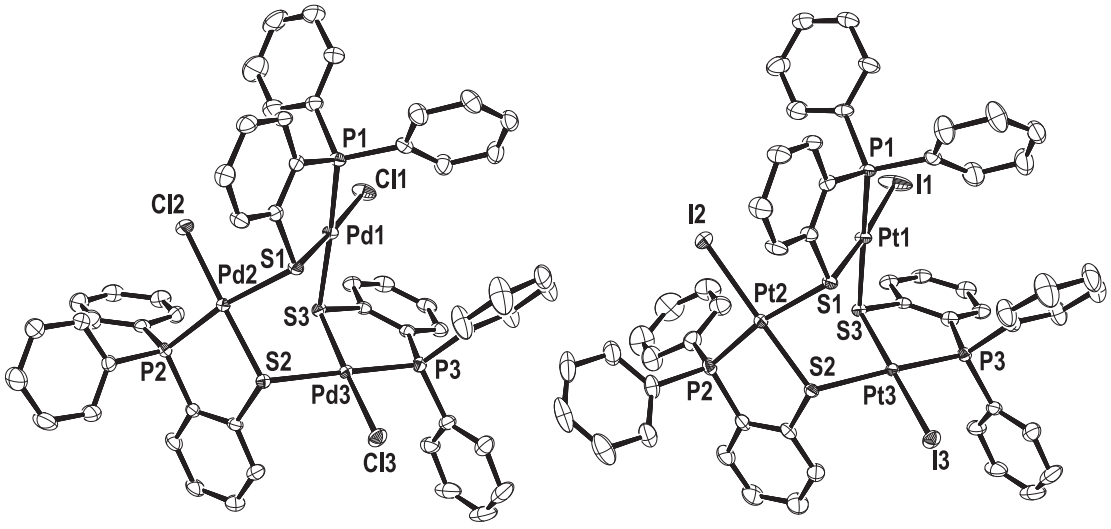

Figure 25. Molecular structures of $[PdCl\{(\mu\text{-}S\text{-}SC_6H_4\text{-}2\text{-}PPh_2)\text{-}\kappa^2S,P\}]_3$ (**7**) and $[PtI\{(\mu\text{-}S\text{-}SC_6H_4\text{-}2\text{-}PPh_2)\text{-}\kappa^2S,P\}]_3$ (**9**). Hydrogen atoms and solvent molecules are omitted for clarity.

The two most similar complexes to **7** and **9** were synthesised by our group: the central fragments of $[PtI\{(\mu\text{-}S\text{-}SC_6H_4\text{-}2\text{-}AsPh_2)\text{-}\kappa^2S,As\}]_3$[56] and $[PtI\{(\mu\text{-}S\text{-}SC_6H_4\text{-}2\text{-}P(Biph)\}\text{-}\kappa^2S,P\}]_3$ (Biph = 1,1'-biphenyl)[94] are comparable with that of complexes **7**

and **9**. However, the distortion of the ring is more pronounced in [PtI{(μ-*S*-SC_6H_4-2-P(Biph))-κ^2*S,P*}]$_3$ due to the greater rigidity introduced by the biphenyl groups.

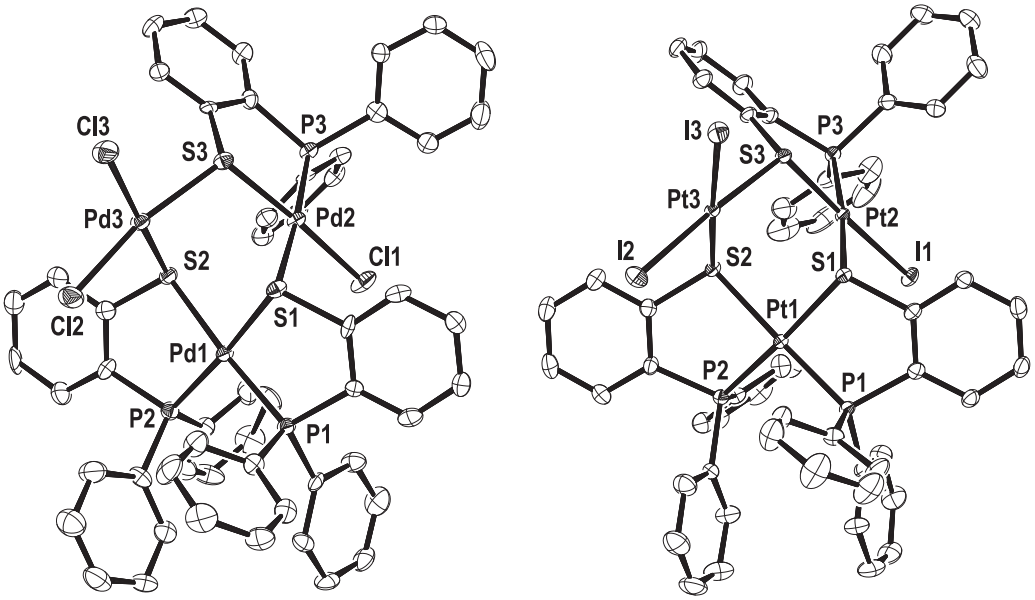

Figure 26. Molecular structures of [(*cis*-Pd{(μ-*S*-SC_6H_4-2-PPh_2)-κ^2*S,P*}$_2$)-$PdCl_2$-PdCl{(μ-*S*-SC_6H_4-2-PPh_2)-κ^2*S,P*}] (**8**) and [(*cis*-Pt{(μ-*S*-SC_6H_4-2-PPh_2)-κ^2*S,P*}$_2$)-PtI_2-PtI{(μ-*S*-SC_6H_4-2-PPh_2)-κ^2*S,P*}] (**10**). Hydrogen atoms and solvent molecules are omitted for clarity.

Table 6. Selected bond lengths and angles for **7** and **9.**

Bond lengths [pm]	**7** (M = Pd)	**9** (M = Pt)	Bond angles [°]	**7** (M = Pd)	**9** (M = Pt)
M(1)–P(1)	223.0(6)	222.8(1)	P(1)–M(1)–S(1)	86.1(2)	86.3(4)
M(1)–S(1)	228.8(6)	230.2(1)	S(1)–M(1)–S(3)	91.2(2)	91.1(4)
M(1)–S(3)	242.5(6)	242.8(1)	P(2)–M(2)–S(2)	86.7(2)	88.2(4)
M(2)–P(2)	223.4(6)	223.6(1)	S(2)–M(2)–S(1)	84.4(2)	81.9(4)
M(2)–S(2)	227.3(5)	227.3(1)	P(3)–M(3)–S(3)	86.5(2)	88.1(4)
M(2)–S(1)	237.3(6)	237.3(1)	S(3)–M(3)–S(2)	93.1(2)	91.6(4)
M(3)–P(3)	223.4(7)	223.5(2)	C(2)–S(1)–M(1)	105.6(8)	105.2(2)
M(3)–S(3)	228.7(6)	228.8(1)	C(20)–S(2)–M(2)	105.4(8)	105.2(2)
M(3)–S(2)	240.5(6)	238.7(1)	C(38)–S(3)–M(3)	105.3(8)	103.8(2)
			M(1)–S(1)–M(2)	97.3(2)	99.8(4)
			M(2)–S(2)–M(3)	105.6(2)	109.7(4)
			M(3)–S(3)–M(1)	103.9(2)	100.4(4)

Table 7. Selected bond lengths and angles for **8** and **10.**

Bond lengths [pm]	**8** (M = Pd)	**10** (M = Pt)	Bond angles [°]	**8** (M = Pd)	**10** (M = Pt)
M(1)–P(2)	225.9(2)	225.3(9)	P(2)–M(1)–P(1)	98.4(7)	99.9(3)
M(1)–P(1)	227.5(2)	225.7(8)	P(2)–M(1)–S(2)	85.6(6)	84.5(3)
M(1)–S(1)	234.6(2)	235.7(8)	P(1)–M(1)–S(1)	84.1(6)	88.9(3)
M(1)–S(2)	233.9(2)	236.1(8)	S(2)–M(1)–S(1)	92.1(6)	91.9(3)
M(2)–P(3)	222.3(2)	222.4(9)	P(3)–M(2)–S(3)	87.7(6)	86.9(3)
M(2)–S(3)	227.6(2)	228.6(8)	S(3)–M(2)–S(1)	86.1(6)	84.7(3)
M(2)–S(1)	237.1(2)	237.8(8)	S(2)–M(3)–S(3)	89.1(6)	87.3(3)
M(3)–S(2)	228.6(2)	230.7(8)	C(2)–S(1)–M(1)	104.6(2)	104.7(1)
M(3)–S(3)	230.7(2)	231.0(8)	M(1)–S(1)–M(2)	92.8(6)	91.4(3)
			C(20)–S(2)–M(1)	104.6(2)	103.1(1)
			M(3)–S(2)–M(1)	102.8 (7)	103.6(3)
			C(38)–S(3)–M(2)	105.0(2)	104.6(1)
			M(2)–S(3)–M(3)	107.5(7)	110.2(3)

4.1.3 Theoretical calculations for Pd (**7**, **8**) and Pt (**9**, **10**) complexes

Independent of the used metal halide in both cases the trimeric forms **7** and **9** are energetically more favoured than their trinuclear counterparts (i.e. **8** and **10**). The relative energy differences between the trinuclear and trimeric forms are very similar: 15.7 kJ mol^{-1} and 10.5 kJ mol^{-1} for **7**/**8** and **9**/**10**, respectively. The trinuclear to trimeric interconversion from **8** to **7** might be facilitated by an intramolecular HOMO-LUMO interaction in **8**. The HOMO of **8** is mainly composed of the Cl(3) lone pair of electrons, which could interact with the σ*(Pd–E) LUMO (E = S, P) located on Pd(1), and trigger the isomeric rearrangement (Figure 27). The HOMO of **10** is composed mainly from the I(2) and I(3) lone pairs of electrons. However, the LUMO of **10** is shared between all three platinum centres, with the highest atomic orbital coefficient located at Pt(2). This might be one of the reasons for the experimentally observed differences between the two isomeric rearrangement reactions. Furthermore, the gas phase Gibbs free energies ($\Delta G°_{gas}$) of the two isomeric rearrangements also suggest the different character of the

two processes. The conversion from **8** to **7**, with $\Delta G°_{gas}$ = –68.5 kJ mol^{-1}, is more exothermic than the isomerisation from **10** to **9** ($\Delta G°_{gas}$ = –36.4 kJ mol^{-1}). The corrections for solvent effects do not alter this trend.

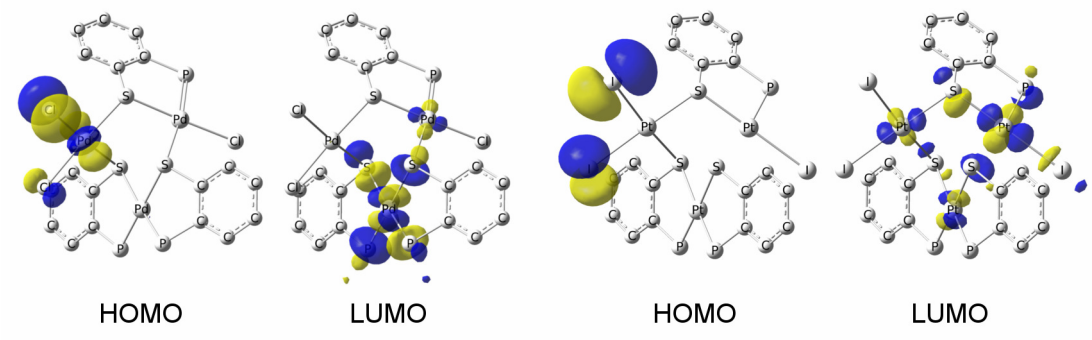

Figure 27. Frontier molecular orbitals of **8** (left) and **10** (right). Hydrogen atoms and terminal phenyl rings are omitted for clarity.

4.2. Coordination chemistry of 1 with metal carbonyl complexes (M = Mo, Mn, Fe)

The reactions of **1** with $[MoCp(CO)_3]_2$, $[Mn_2(CO)_{10}]$, $[Fe(CO)_5]$ and $[FeCp(CO)_2]_2$ led to the complexes presented on scheme 28. The formation of compounds **11**–**15** presumes the scission of the M–M bond of the starting dimeric carbonyl complexes, and all the reactions feature the cleavage of the As–S bond of **1**. In compounds **11**, **14** and **15** the coordination of the resulting phosphanylthiolato ligand to one metal centre can be observed. $[Mn_2(CO)_7(\mu\text{-}AsPh_2)\{(SC_6H_4\text{-}2\text{-}PPh_2)\text{-}\kappa S,P\}]$ (**12**) is the only reaction product with **1** which contains all three donor atoms in its structure. The cleaved $AsPh_2$ group is included in the final complex and bridges two Mn atoms, while the P,S chelating pocket coordinates to one Mn centre. At the same time $[Mn_2(CO)_8(\mu\text{-}AsPh_2)_2]$ (**13**) serves as the single example where the metal centres are coordinated only by bridging $AsPh_2$ groups and the $(SC_6H_4\text{-}2\text{-}PPh_2)^-$ part of the ligand is excluded.

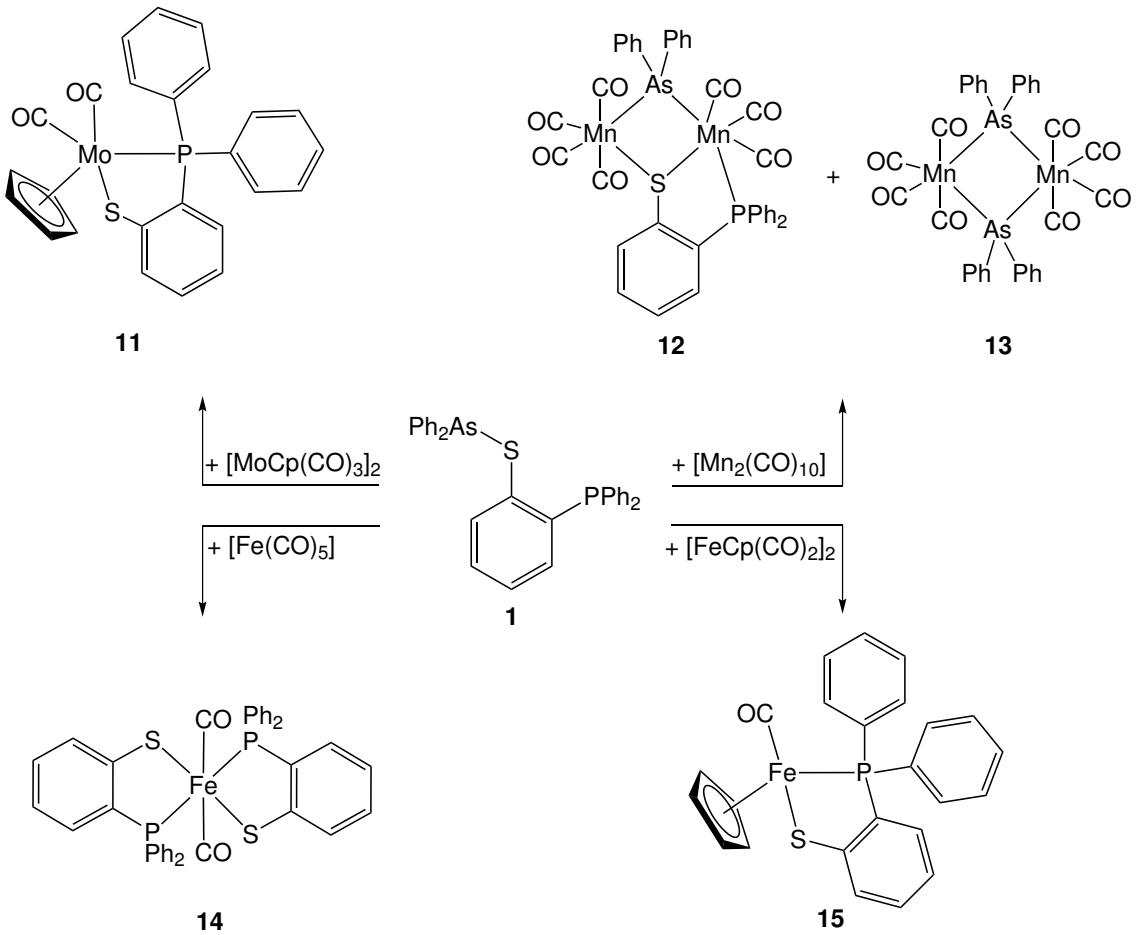

Scheme 28. Reaction of **1** with metal carbonyl complexes.

The [MoCp(CO)$_2${(SC$_6$H$_4$-2-PPh$_2$)-κ*S*,*P*}] (**11**) complex crystallises in the monoclinic space group $P2_1/n$ with four molecules in the unit cell. The molecular structure is depicted on Figure 28.

Compound **11** is formed by coordination of the phosphanylthiolato ligand to one Mo atom giving a five-membered MoSC$_2$P ring. The molybdenum atom is in a square-pyramidal environment with the four basal positions being occupied by two *cis*-orientated carbonyl ligands, the diphenylphosphanido group and the sulfur atom. In addition, the apical position is occupied by a cyclopentadienyl ligand. Phosphorus is coordinated in a tetrahedral fashion. The conformation adopted by the phenyl rings minimises the steric effects between them and the cyclopentadienyl ring. Selected bond lengths and angles for complex **11** are presented in Table 8.

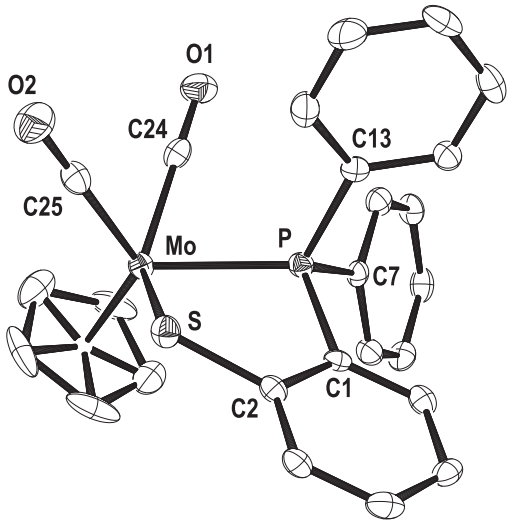

Figure 28. Molecular structure of [MoCp(CO)$_2${(SC$_6$H$_4$-2-PPh$_2$)-κ*S*,*P*}] (**11**). Hydrogen atoms are omitted for clarity.

Table 8. Selected bond lengths and angles for **11**.

Bond lengths [pm]		Bond angles [°]	
Mo(1)–P(1)	244.8(5)	P(1)–Mo(1)–S(1)	74.8(2)
Mo(1)–S(1)	251.1(5)	Mo(1)–P(1)–C(1)	109.7(6)
Mo(1)–C(24)	195.9(2)	Mo(1)–S(1)–C(2)	107.0(7)
Mo(1)–C(25)	196.4(2)	C(24)–Mo(1)–C(25)	75.7(9)

The molecular structures of [Mn$_2$(CO)$_7$(μ-AsPh$_2$){(SC$_6$H$_4$-2-PPh$_2$)-κ*S*,*P*}] (**12**) and [Mn$_2$(CO)$_8$(μ-AsPh$_2$)$_2$] (**13**) are presented in Figure 29 and Figure 30. Complex **12** crystallises in the monoclinic space group *C*2/c with eight molecules in the unit cell. The two manganese atoms are bridged by the AsPh$_2$ group and through the S atom. In addition, P coordinates to one of the Mn atoms giving a five-membered Mn(1)SC$_2$P ring. Mn(1) is additionally ligated by three, Mn(2) by four carbonyl groups. Each manganese atom is coordinated in an approximately octahedral fashion. The long Mn···Mn distance of 372 pm indicates the absence of a bonding interaction between the two metal centres (Table 9).

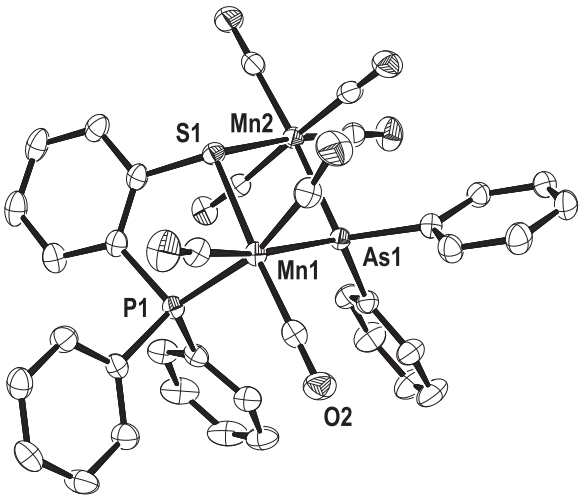

Figure 29. Molecular structure of $[Mn_2(CO)_7(\mu\text{-}AsPh_2)\{(SC_6H_4\text{-}2\text{-}PPh_2)\text{-}\kappa S,P\}]$ (**12**). Hydrogen atoms are omitted for clarity.

Table 9. Selected bond lengths and angles for **12**.

Bond lengths [pm]		Bond angles [°]	
Mn(1)–As(1)	248.3(4)	Mn(1)–As(1)–Mn(2)	97.2(1)
Mn(1)–S(1)	229.7(6)	Mn(1)–S(1)–Mn(2)	102.0(2)
Mn(1)–P(1)	236.9(6)	S(1)–Mn(1)–As(1)	80.7(2)
Mn(1)–C(31)	180.5(2)	S(1)–Mn(2)–As(1)	80.1(2)
Mn(1)–C(32)	180.2(2)	Mn(1)–S(1)–C(2)	105.8(7)
Mn(1)–C(33)	181.9(2)	Mn(1)–P(1)–C(1)	107.1(8)
Mn(2)–As(1)	247.2(4)	P(1)–Mn(1)–C(33)	165.9(8)
Mn(2)–S(1)	241.6(6)	As(1)–Mn(1)–C(31)	170.3(8)
Mn(2)–C(34)	185.0(2)	S(1)–Mn(1)–C(32)	173.7(7)
Mn(2)–C(35)	180.9(2)	C(34)–Mn(2)–C(36)	175.5(9)
Mn(2)–C(36)	186.1(2)	As(1)–Mn(2)–C(37)	172.2(8)
Mn(2)–C(37)	183.2(2)	S(1)–Mn(2)–C(35)	173.7(7)

In complex **13** the two manganese atoms are bridged by two $AsPh_2$ groups, adopting a “butterfly” conformation, and each metal centre is ligated by four carbonyl groups. This completes an approximately octahedral arrangement about each manganese

atom. The length of the Mn···Mn distance of 384 pm indicates no metal-metal bonding (Table 10).

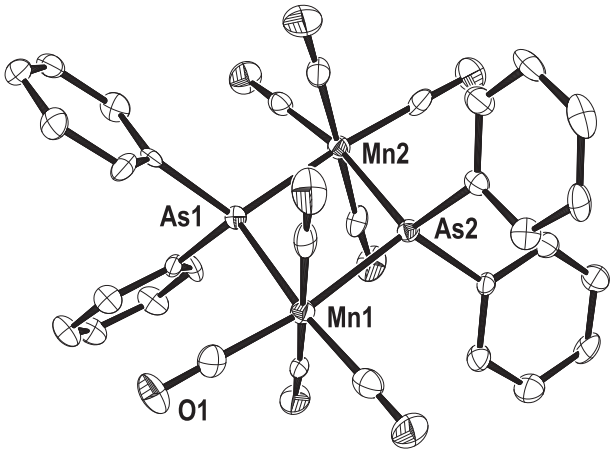

Figure 30. Molecular structure of $[Mn_2(CO)_8(\mu\text{-}AsPh_2)_2]$ (**13**). Hydrogen atoms are omitted for clarity.

Table 10. Selected bond lengths and angles for **13**.

Bond lengths [pm]		Bond angles [°]	
Mn(1)–As(1)	245.9(9)	Mn(1)–As(1)–Mn(2)	102.4(3)
Mn(2)–As(1)	246.5(9)	Mn(1)–As(2)–Mn(2)	101.8(3)
Mn(1)–As(2)	247.0(9)	As(1)–Mn(1)–As(2)	77.9(3)
Mn(2)–As(2)	247.5(9)	As(1)–Mn(2)–As(2)	77.7(3)
		C(26)–Mn(1)–C(27)	172.8(2)
		C(30)–Mn(2)–C(31)	176.8(2)

$[Fe(CO)_2\{(SC_6H_4\text{-}2\text{-}PPh_2)\text{-}\kappa^2S,P)\}_2]$ (**14**) crystallises in the monoclinic space group $P2_1/n$ with two molecules in the unit cell. The molecule of **14** is located on a special position, a centre of inversion. The Fe atom is coordinated in an octahedral fashion by two carbonyl groups and two chelating P,S ligands. The ligands adopt a *trans* arrangement upon coordination to the metal centre. The phosphorus atoms are coordinated in a tetrahedral fashion by the carbon atoms of the phenyl rings and the iron atom. Selected bond lengths and angles for the complex are presented in Table 11.

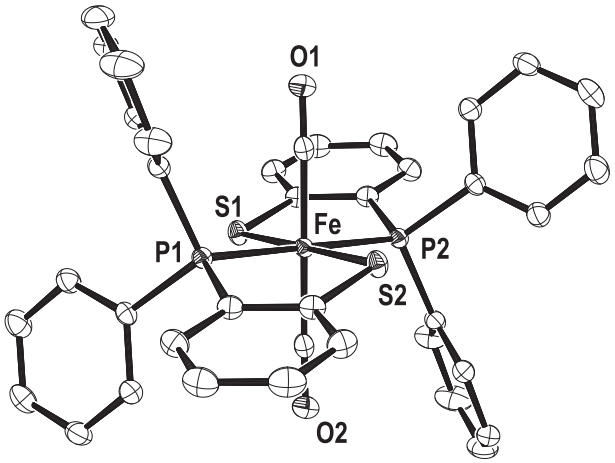

Figure 31. Molecular structure of $[Fe(CO)_2\{(SC_6H_4\text{-}2\text{-}PPh_2)\text{-}\kappa^2S,P)\}_2]$ (**14**). Hydrogen atoms and solvent molecules are omitted for clarity.

Table 11. Selected bond lengths and angles for **14**.

Bond lengths [pm]		Bond angles [°]	
Fe–P(1)	223.5(4)	P(1)–Fe–S(2)	86.6(2)
Fe–P(2)	223.5(4)	S(2)–Fe–P(2)	93.4(2)
Fe–S(2)	230.9(3)	P(2)–Fe–S(1)	86.6(2)
Fe–S(1)	230.9(3)	S(1)–Fe–P(1)	93.4(2)
Fe–C(1)	180.8(2)	C(1)–Fe–C(2)	180.0
Fe–C(2)	180.8(2)		

The molecular structure of $[FeCp(CO)\{(SC_6H_4\text{-}2\text{-}PPh_2)\text{-}\kappa S,P\}]$ (**15**) is presented in Figure 31. Complex **15** crystallises in the monoclinic space group *I*2/a with eight molecules in the unit cell. The iron atom is in a trigonal-pyramidal environment with the three basal positions being occupied by a carbonyl ligand, the diphenylphosphanido group and the sulfur atom. In addition, the apical position is occupied by a cyclopentadienyl ligand. Phosphorus is coordinated in a tetrahedral fashion. The overall molecular structure of **15** resembles that of compound **11**. Selected bond lengths and angles for **15** are presented in Table 12.

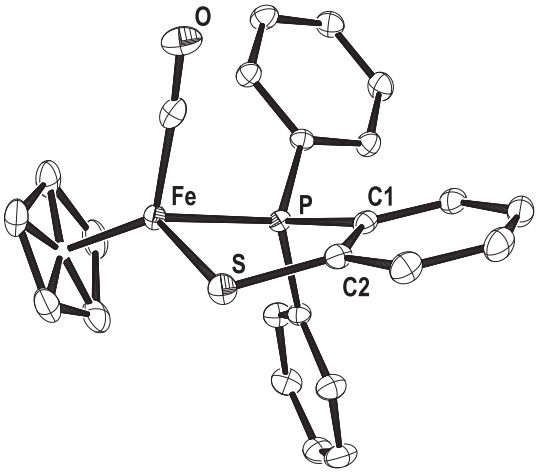

Figure 32. Molecular structure of [FeCp(CO){(SC_6H_4-2-PPh_2)-κ*S*,*P*}] (**15**). Hydrogen atoms are omitted for clarity.

Table 12. Selected bond lengths and angles for **15**.

Bond lengths [pm]		Bond angles [°]	
Fe(1)–P(1)	217.1(4)	P(1)–Fe(1)–S(1)	85.2(2)
Fe(1)–S(1)	227.6(5)	Fe(1)–P(1)–C(1)	107.8(5)
Fe(1)–C(24)	174.5(2)	Fe(1)–S(1)–C(2)	104.1(5)

5. Coordination chemistry of SPAs (3) with rhodium and group 10 metal(II) complexes

5.1. Synthesis and molecular structure of [$RhCl_2${(Rh(cod)(SC_6H_3-2-PPh_2-3-$AsPh_2$)-κ*S*,*P*)-κ*S*,*As*}$_2$][$RhCl_2$(cod)] (16)

Treatment of two equivalents of **SPAs** with 1.5 equivalents of $[RhCl(cod)]_2$ in THF resulted in the formation of the trinuclear cationic rhodium complex [$RhCl_2${(Rh(cod)(SC_6H_3-2-PPh_2-3-$AsPh_2$)-κ*S*,*P*)-κ*S*,*As*}$_2$][$RhCl_2$(cod)] (**16**). The $^{31}P\{^1H\}$ NMR of compound **16** shows two doublets at δ = 59.6 (d, $J_{P,Rh}$ = 145 Hz) and

46.3 (d, $J_{P,Rh}$ = 105 Hz), indicating two non-equivalent P atoms which show coupling with the Rh centres. Compound **16** crystallises in the monoclinic space group $P2_1/c$ with four cations and four anions in the unit cell. The molecular structure is shown in Figure 33, selected bond lengths and angles are listed in Table 13.

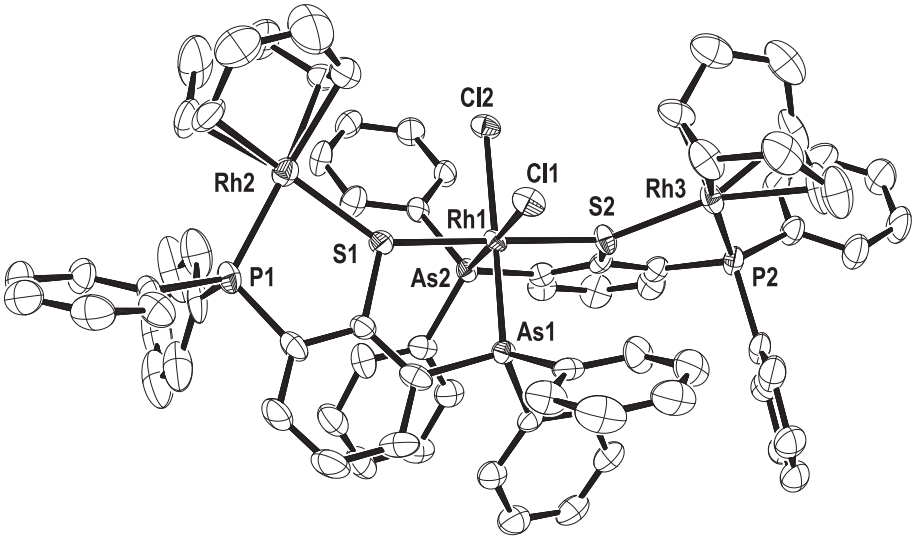

Figure 33. Molecular structure of the cation $[RhCl_2\{(Rh(cod)(SC_6H_3\text{-}2\text{-}PPh_2\text{-}3\text{-}AsPh_2)\text{-}\kappa S,P)\text{-}\kappa S,As\}_2]^+$ in **16**. Hydrogen atoms, solvent molecules and the $[RhCl_2(cod)]^-$ anion are omitted for clarity.

Table 13. Selected bond lengths and angles for **16**.

Bond lengths [pm]		Bond angles [°]			
Rh(1)–As(1)	233.4(1)	As(2)–Rh(1)–As(1)	96.1(4)	S(1)–Rh(1)–Cl(2)	91.6(7)
Rh(1)–As(2)	232.8(1)	As(2)–Rh(1)–S(1)	93.3(6)	S(2)–Rh(1)–Cl(2)	88.5(7)
Rh(1)–S(1)	235.2(2)	As(1)–Rh(1)–S(1)	86.3(6)	Cl(1)–Rh(1)–Cl(2)	89.0(7)
Rh(1)–S(2)	235.5(2)	As(2)–Rh(1)–S(2)	85.8(6)	P(1)–Rh(2)–S(1)	82.1(6)
Rh(1)–Cl(1)	239.6(2)	As(1)–Rh(1)–S(2)	93.7(6)	P(2)–Rh(3)–S(2)	83.1(6)
Rh(1)–Cl(2)	239.8(2)	S(1)–Rh(1)–S(2)	179.1(8)	C(2)–S(1)–Rh(2)	109.0(3)
Rh(2)–P(1)	230.6(1)	As(2)–Rh(1)–Cl(1)	177.2(6)	C(2)–S(1)–Rh(1)	107.5(3)
Rh(2)–S(1)	233.4(2)	As(1)–Rh(1)–Cl(1)	86.6(6)	C(32)–S(2)–Rh(3)	107.8(3)
Rh(3)–P(2)	231.6(1)	S(1)–Rh(1)–Cl(1)	87.7(7)	C(32)–S(2)–Rh(1)	108.2(3)
Rh(3)–S(2)	231.6(2)	S(2)–Rh(1)–Cl(1)	93.2(7)	Rh(2)–S(1)–Rh(1)	143.1(9)
		As(2)–Rh(1)–Cl(2)	88.3(6)	Rh(3)–S(2)–Rh(1)	142.3(9)
		As(1)–Rh(1)–Cl(2)	175.3(6)		

The X-ray structure analysis of **16** shows a cationic trinuclear rhodium complex with two bridging sulfur atoms from two **SPAs**$^-$ ligands. The central rhodium(III) atom is coordinated in an octahedral fashion by two As, two S and two terminal Cl atoms. Since these ligands act as two-, two- and one-electron donors, respectively, the central Rh atom has 18 valence electrons. The two terminal rhodium(I) atoms are coordinated in a square-planar fashion by the P and S donors of the **SPAs**$^-$ ligands and a 1,5-cyclooctadiene molecule. In this case the P, S and COD ligands act as two-, one- and four-electron donors, respectively, and each rhodium(I) atom has 16 valence electrons. Thus, the structure shows four five-membered metallacycles: two PCCSRh and two AsCCSRh rings.

5.2. Synthesis and molecular structure of *trans*-[Ni{(SC_6H_3-2-PPh_2-3-$AsPh_2$)-κ^2*S,P*}$_2$] (17)

The complex *trans*-[Ni{(SC_6H_3-2-PPh_2-3-$AsPh_2$)-κ^2*S,P*)}$_2$] (**17**) was obtained from the reaction of **SPAs** with [$NiCl_2 \cdot 6H_2O$] in THF. No formation of a bimetallic complex was detected when the reaction was repeated using different ratios of the reagents (ligand/metal, 2:1, 1:1, and 1:2), **17** was always isolated as the major product.

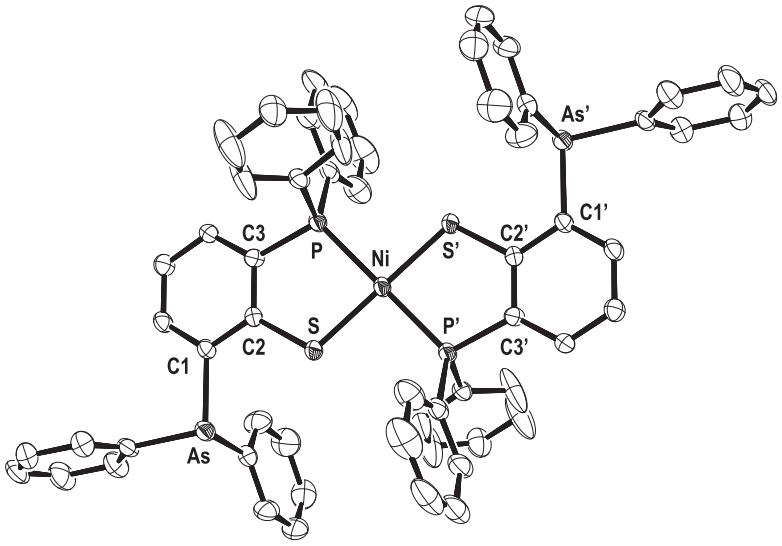

Figure 34. Molecular structure of *trans*-[Ni{(SC_6H_3-2-PPh_2-3-$AsPh_2$)-κ^2*S,P*}$_2$] (**17**). Hydrogen atoms and solvent molecules are omitted for clarity.

Compound **17** crystallises in the triclinic space group $P\bar{1}$ with one molecule in the unit cell. The molecular structure is shown on Figure 34, selected bond lengths and angles are listed in Table 14. **17** is a mononuclear complex which contains two identical ligands coordinating through their P,S chelating pocket to the metal centre in a *trans* arrangement. The structure shows the nickel atom located at a crystallographic inversion centre. Bond angles between adjacent donor atoms are very close to the theoretical 90° value.

Table 14. Selected bond lengths and angles for **17**.

Bond lengths [pm]		Bond angles [°]	
Ni–S	217.0(1)	S–Ni–P	88.4(4)
Ni–P	218.2(1)	S'–Ni–P	91.6(4)
S–C(2)	177.2(4)	P–Ni–P'	180.0(1)
P–C(3)	179.8(4)	C(2)–S–Ni	106.7(1)
		C(3)–P–Ni	107.7(1)

5.3. Synthesis and molecular structure of [{$Pd_2Cl_2(SC_6H_3$-2-PPh_2-3-$AsPh_2$)}$_2$(μ-Cl)$_2$] (18)

Treatment of **SPAs** with 2 equivalents of [$PdCl_2$(cod)] in THF resulted in formation of the tetranuclear platinum complex [{$Pd_2Cl_2(SC_6H_3$-2-PPh_2-3-$AsPh_2$)}$_2$(μ-Cl)$_2$] (**18**). The symmetry of the complex is proved by the $^{31}P\{^1H\}$ NMR spectrum, which exhibits a singlet at δ = 53.1, indicating two magnetically equivalent phosphorus atoms. Compound **18** crystallises in the monoclinic space group *P*2/n with two independent molecules in the asymmetric unit. Both molecules are located on a special position (C_2-axis). The X-ray crystal structure determination revealed the formation of the dimeric tetranuclear complex **18** (Figure 35) showing four intramolecular five-membered rings formed by the coordination of the E,S chelating groups to the palladium centres, and one central eight-membered ring formed by connection of the two dinuclear fragments via chloride bridges. The nearly square-planar coordination

environment around each palladium centre is completed by one terminal and one bridging chloro ligand (Table 15).

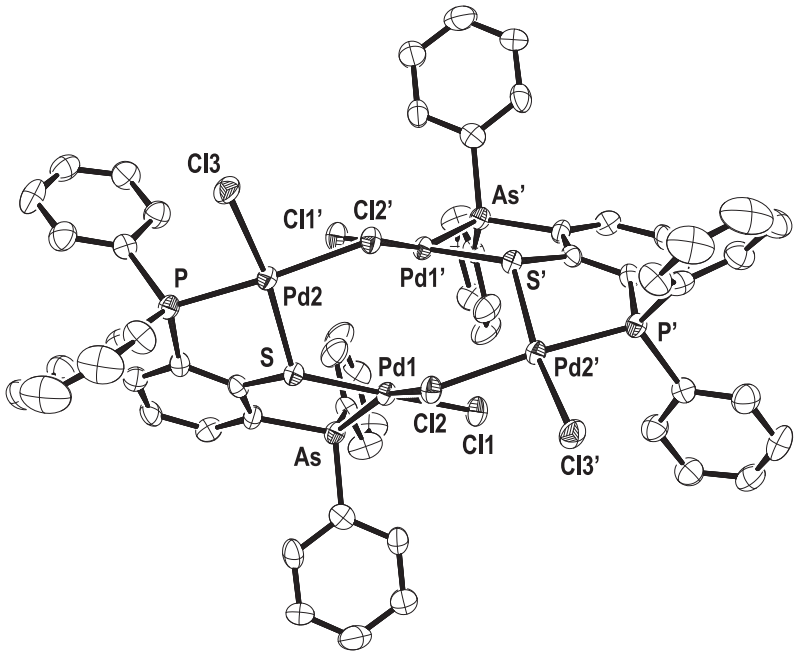

Figure 35. Molecular structure of $[\{Pd_2Cl_2(SC_6H_3\text{-}2\text{-}PPh_2\text{-}3\text{-}AsPh_2)\}_2(\mu\text{-}Cl)_2]$ (**18**). Hydrogen atoms and solvent molecules are omitted for clarity.

Table 15. Selected bond lengths and angles for **18**.

Bond lengths [pm]		Bond angles [°]	
Pd(1)–As(1)	229.4(1)	As(1)–Pd(1)–Cl(2)	157.3(6)
Pd(1)–S(1)	226.6(2)	S(1)–Pd(1)–Cl(1)	178.0(8)
Pd(2)–P(1)	225.5(2)	S(1)–Pd(2)–Cl(3)	168.0(8)
Pd(2)–S(1)	228.9(2)	Cl(2)–Pd(2)–P(1)	173.1(7)
Pd(1)–Cl(1)	231.6(2)	Pd(1)–S(1)–Pd(2)	122.7(9)
Pd(1)–Cl(2)	240.1(2)	Pd(2)–Cl(2)–Pd(1)	111.3(8)
Pd(2)–Cl(3)	231.0(2)		
Pd(2)–Cl(2)	236.9(2)		

5.4. Synthesis and molecular structure of *cis*-[Pt{(SC_6H_3-2-PPh_2-3-$AsPh_2$)-κ^2*S,P*}$_2$] (19a)

The 2:1 reaction of **SPAs** and [PtI_2(cod)] in THF resulted in the mononuclear complex *cis*-[Pt{(SC_6H_3-2-PPh_2-3-$AsPh_2$)-κ^2*S,P*}$_2$] (**19a**). The $^{31}P\{^1H\}$ NMR spectrum of the reaction media showed two singlets with the appropriate satellites at δ = 48.7 ($J_{P,Pt}$ = 2642 Hz) and δ = 40.8 ($J_{P,Pt}$ = 2901 Hz) (**19a**). The first shift was assumed to be *trans*-[Pt{(SC_6H_3-2-PPh_2-3-$AsPh_2$)-κ^2*S,P*}$_2$] (**19b**), which in solution converts into the thermodynamically more stable *cis* isomer. The isomerisation process was monitored by $^{31}P\{^1H\}$ NMR spectroscopy, at room temperature full conversion takes approximately two weeks. Compound **19a** crystallises in the triclinic space group $P\bar{1}$ with two molecules in the unit cell. The molecular structure is shown in Figure 38, selected bond lengths and angles are listed in Table 16. Compound **19a** is a mononuclear complex which contains two identical ligands coordinating through their P,S chelating pockets to the metal centre in a *cis* arrangement. The Pt centre is located in a slightly distorted square-planar environment (Table 16), due to the steric effects.

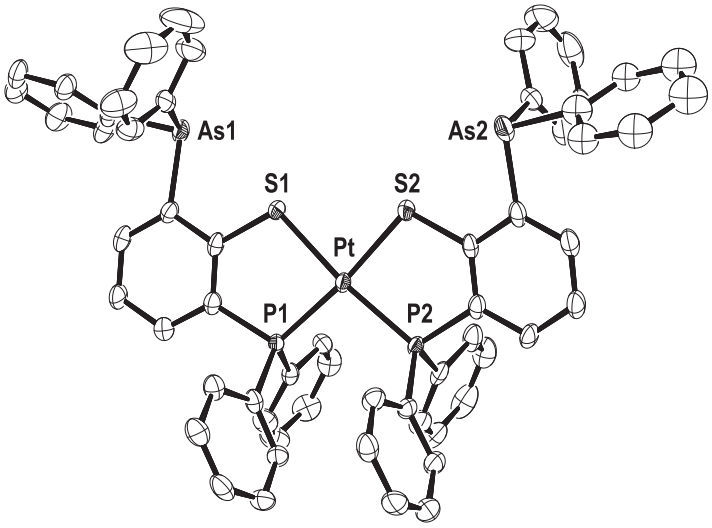

Figure 38. Molecular structure of *cis*-[Pt{(SC_6H_3-2-PPh_2-3-$AsPh_2$)-κ^2*S,P*}$_2$] (**19a**). Hydrogen atoms and solvent molecules are omitted for clarity.

Table 16. Selected bond lengths and angles for **19a**.

Bond lengths [pm]		Bond angles [°]	
Pt(1)–P(1)	224.4(1)	P(2)–Pt(1)–S(1)	173.6(5)
Pt(1)–P(2)	224.8(1)	P(1)–Pt(1)–S(2)	173.9(4)
Pt(1)–S(2)	231.2(1)	P(1)–Pt(1)–P(2)	98.6(5)
Pt(1)–S(1)	231.8(1)	S(1)–Pt(1)–S(2)	86.6(5)

5.5. Synthesis and molecular structure of [Pt{(PtI_2(SC_6H_3-2-PPh_2-3-$AsPh_2$)-κ*S*,*P*)-κ*S*,*As*}$_2$] (20)

Treatment of two equivalents of **SPAs** with three equivalents of [PtI_2(cod)] in THF resulted in formation of the trinuclear platinum complex [Pt{(PtI_2(SC_6H_3-2-PPh_2-3-$AsPh_2$)-κ*S*,*P*)-κ*S*,*As*}$_2$] (**20**). The three platinum centres are bridged *via* the sulfur atoms of two **SPAs**$^-$ ligands. The $^{31}P\{^1H\}$ NMR spectrum of compound **20** shows a singlet at δ = 39.2 with the corresponding satellites ($J_{P,Pt}$ = 3293 Hz), due to P-Pt coupling. Compound **20** crystallises in the monoclinic space group $P2_1/n$ with four molecules in the unit cell. The molecular structure of **20** is shown in Figure 39, selected bond lengths and angles are listed in Table 17.

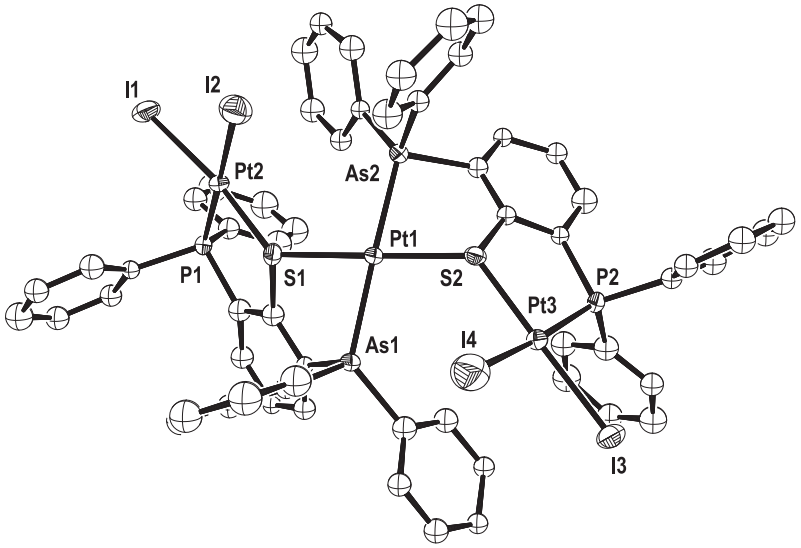

Figure 39. Molecular structure of [Pt{(PtI_2(SC_6H_3-2-PPh_2-3-$AsPh_2$)-κ*S*,*P*)-κ*S*,*As*}$_2$] (**20**). Hydrogen atoms and solvent molecules are omitted for clarity.

The central unit of the complex is formed by the coordination of two As, S donor atoms at Pt(1) in a *trans* arrangement. The Pt(2) and Pt(3) centres are chelated by the P, S donor atoms, and the coordination sphere around them is completed by two iodo ligands to give an approximately square-planar geometry.

Table 17. Selected bond lengths and angles for **20.**

Bond lengths [pm]		Bond angles [°]			
Pt(1)–S(2)	232.4(5)	S(2)–Pt(1)–S(1)	177.2(2)	P(2)–Pt(3)–S(2)	89.1(2)
Pt(1)–S(1)	234.4(5)	S(2)–Pt(1)–As(2)	80.6(1)	P(2)–Pt(3)–I(4)	171.3(2)
Pt(1)–As(2)	240.1(2)	S(1)–Pt(1)–As(2)	99.4(2)	S(2)–Pt(3)–I(4)	88.1(1)
Pt(1)–As(1)	241.2(2)	S(2)–Pt(1)–As(1)	100.6(2)	P(2)–Pt(3)–I(3)	91.1(2)
Pt(2)–P(1)	222.4(6)	S(1)–Pt(1)–As(1)	79.8(2)	S(2)–Pt(3)–I(3)	178.6(2)
Pt(2)–S(1)	226.6(6)	As(2)–Pt(1)–As(1)	172.3(8)	I(4)–Pt(3)–I(3)	91.6(7)
Pt(2)–I(1)	259.4(2)	P(1)–Pt(2)–S(1)	88.9(2)		
Pt(2)–I(2)	261.9(2)	P(1)–Pt(2)–I(1)	90.7(2)		
Pt(3)–P(2)	222.2(5)	S(1)–Pt(2)–I(1)	171.2(1)		
Pt(3)–S(2)	227.9(6)	P(1)–Pt(2)–I(2)	176.3(2)		
Pt(3)–I(4)	257.5(2)	S(1)–Pt(2)–I(2)	89.2(2)		
Pt(3)–I(3)	261.9(2)	I(1)–Pt(2)–I(2)	90.7(7)		

5.6. Theoretical study of the *cis-trans* isomerism of 17 and 19a.

In order to infer the effect of the substituents on the relative stability of these systems, energy data calculated at the same level of theory for the model compounds [M{(S-C_6H_3-2-PH_2-3-AsH_2)-$\kappa^2 S,P$}$_2$] (Scheme 37) was also calculated.

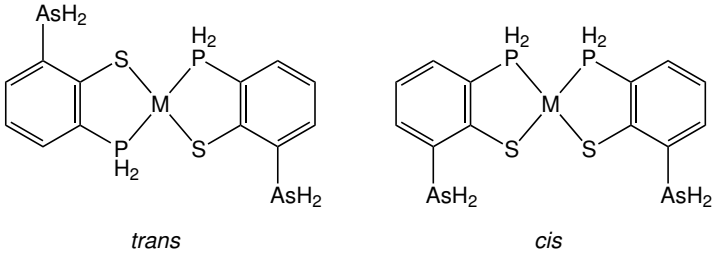

trans *cis*

Scheme 37. Model systems for [M{(**SPAs**)-$\kappa^2 S,P$}$_2$], M = Ni, Pt.

All calculations were carried out with the same setup (see chapter 8.3 for details) as in a similar theoretical study done by our group,[94] in order to compare results between [M{(**SPAs**)-κ^2*S,P*}$_2$] (M = Ni, Pt) and the related [M{(**BiphPS**)-κ^2*S,P*}$_2$] (M = Ni, Pt) complexes. The *cis-trans* relative energies (ΔE) for [M{(**SPAs**)-κ^2*S,P*}$_2$] decreases on going from Ni to Pt, but ΔE of the corresponding model complexes is lower than ΔE for the real systems and the *trans* isomer is energetically always more favoured than the *cis* forms, for both real and model system (Figure 41).

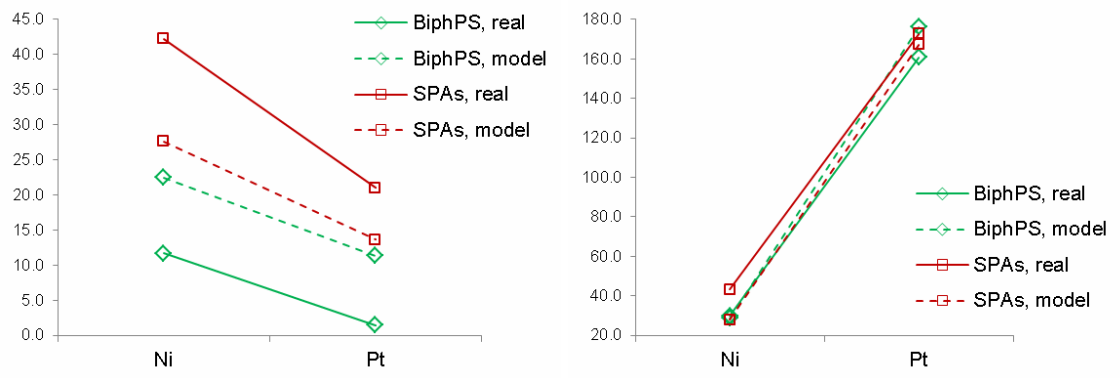

Figure 41. Variations in *trans/cis* relative energies (left) and singlet-triplet splitting energies (right) for [M{(**SPAs**)-κ^2*S,P*}$_2$] (shown in red) and [M{(**BiphPS**)-κ^2*S,P*}$_2$] (shown in green, values taken from ref. 94). M = Ni, Pt; values are in kJ mol^{-1}.

This clearly explains why for the nickel complexes only the *trans* isomer (**17**) was observed experimentally. However, for the platinum analogues, the intramolecular π-π interactions might favour the formation of the corresponding *cis* isomer (**19a**). In the case of [M{(**SPAs**)-κ^2*S,P*}$_2$], the singlet-triplet (S-T) separation for the model compounds are lower than for the real systems, indicating that the substituents on phosphorus enhance the barrier of the *cis-trans* interconversion (relative to the model).

The ΔE and S-T trends of the [M{(**SPAs**)-κ^2*S,P*}$_2$] model and real systems are the opposite of the trends observed for the [M{(**BiphPS**)-κ^2*S,P*}$_2$] complexes. Our previous theoretical study on the [M{(**BiphPS**)-κ^2*S,P*}$_2$] system showed, that both ΔE and S-T separation of the model compounds are higher than ΔE and S-T separation of the real systems.[94] These trends are reversed for the [M{(**SPAs**)-κ^2*S,P*}$_2$] systems, indicateing a difference between the strength of the possible π-π interactions between the two different types of ligands. It seems that the π-π interactions between the phenyl

rings of two **SPAs** units are weaker than the π-π interactions between the phenyl rings of two more rigid **BiphPS** moieties, but still strong enough to induce the formation of the thermodynamically unfavoured *cis* isomer for the platinum [M{(**SPAs**)-κ^2*S,P*}$_2$] complex.

6. Coordination chemistry of *trans*-[Ni{(SC_6H_3-2-PPh_2-3-$AsPh_2$)-κ^2*S,P*}$_2$] (17) with group 10 metal(II) complexes

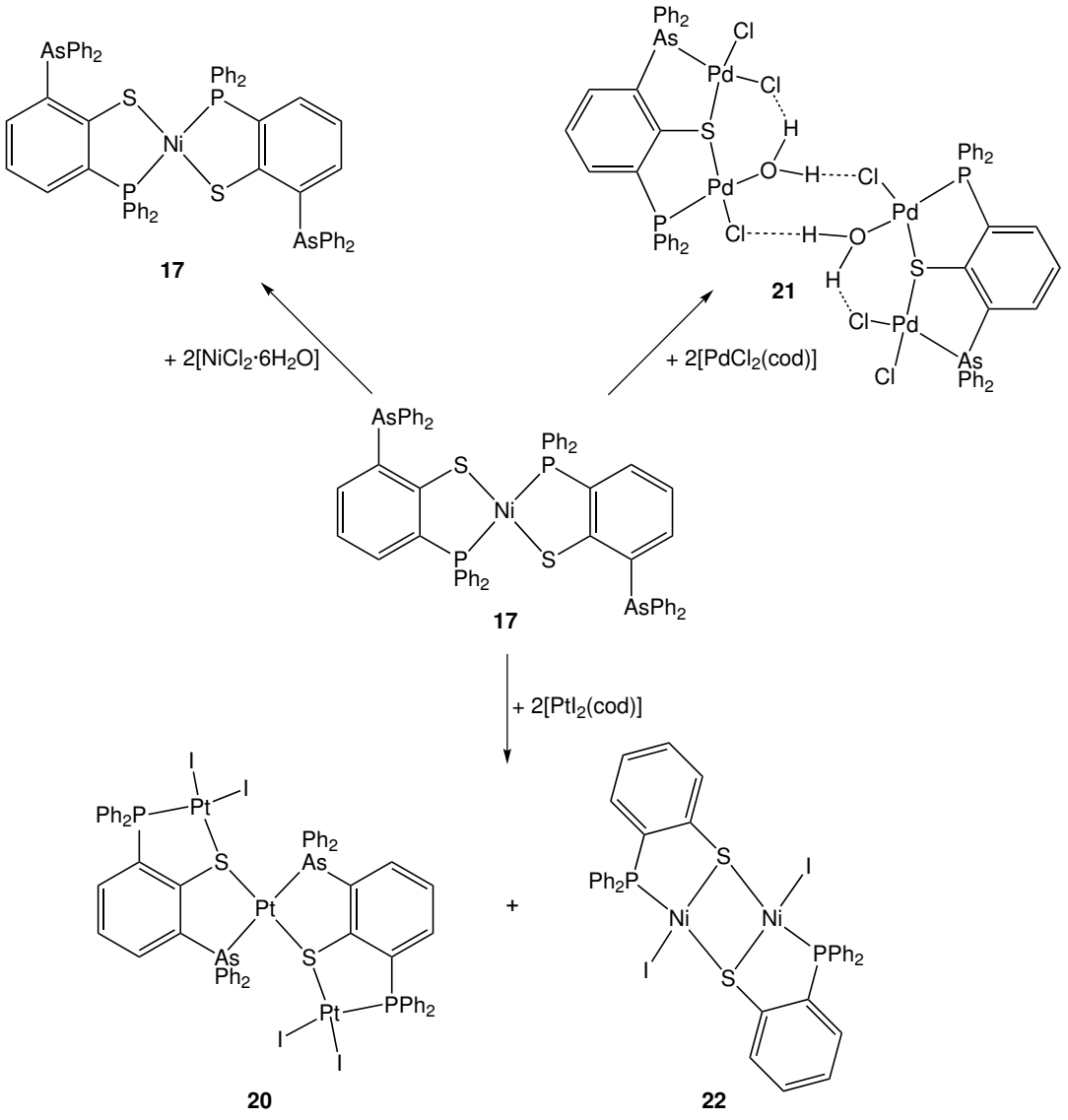

Scheme 38. Reaction of **17** with group 10 metal(II) complexes.

Compound **17** exhibits two $AsPh_2$ groups still available for further coordination. Therefore, its reaction with $NiCl_2 \cdot 6H_2O$, $[PdCl_2(cod)]$ and $[PtI_2(cod)]$ in THF, in a 1:2 ratio, was investigated (Scheme 38). The reaction with $NiCl_2 \cdot 6H_2O$, however, did not take place, nor at room temperature (THF, 48 h) or at reflux conditions (toluene, 24 h). Reaction of **17** with $[PdCl_2(cod)]$ conducted at room temperature in THF gave almost insoluble brownish microcrystals, which proved to be $[\{Pd_2Cl_2(OH_2)(SC_6H_3\text{-}2\text{-}PPh_2\text{-}3\text{-}AsPh_2)\}_2]$ (**21**). Compound **21** crystallises in the monoclinic space group $P2_1/c$ with four molecules in the unit cell. The molecular structure is shown in Figure 42, selected bond lengths and angles are listed in Table 19. The X-ray diffraction analysis revealed a dimeric structure showing four intramolecular five-membered rings formed by coordination of the E,S chelating compartments to the palladium centres. The nearly square-planar coordination environment around Pd(1) is completed by two chloro ligands, and around Pd(2) by one chloro ligand and one water molecule. Water is coordinating *trans* to phosphorus. Thus, two monomeric units are held together via two intermolecular hydrogen bonds between water and a chloro ligand.

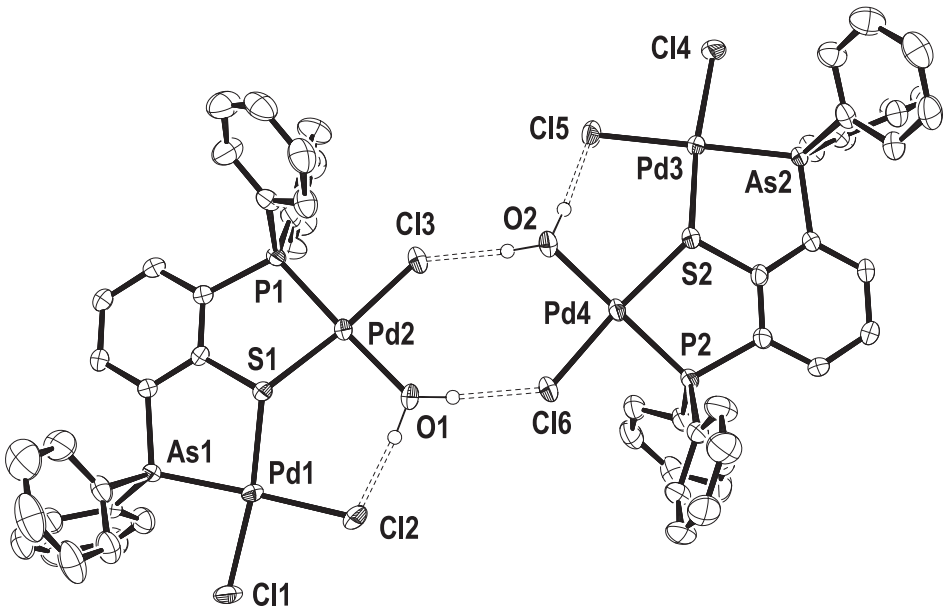

Figure 42. Molecular structure of $[\{Pd_2Cl_2(OH_2)(SC_6H_3\text{-}2\text{-}PPh_2\text{-}3\text{-}AsPh_2)\}_2]$ (**21**). Aryl hydrogen atoms and solvent molecules are omitted for clarity.

Table 19. Selected bond lengths and angles for **21**.

Bond lengths [pm]		Bond angles [°]	
Pd(1)–As(1)	227.8(5)	As(1)–Pd(1)–Cl(2)	176.9(4)
Pd(1)–S(1)	229.3(9)	S(1)–Pd(1)–Cl(1)	170.5(4)
Pd(2)–P(1)	223.1(7)	S(1)–Pd(2)–Cl(3)	173.6(4)
Pd(2)–S(1)	229.0(8)	O(1)–Pd(2)–P(1)	175.8(2)
Pd(3)–As(2)	230.3(4)	As(2)–Pd(3)–Cl(5)	178.0(3)
Pd(3)–S(2)	228.3(9)	S(2)–Pd(3)–Cl(4)	169.8(3)
Pd(4)–P(2)	222.6(8)	S(2)–Pd(4)–Cl(6)	171.96(4)
Pd(4)–S(2)	226.6(8)	O(2)–Pd(4)–P(2)	176.1(8)
Pd(1)–Cl(1)	231.3(9)	Pd(4)–S(2)–Pd(3)	132.9(4)
Pd(1)–Cl(2)	234.8(1)	Pd(2)–S(1)–Pd(1)	128.5(4)
Pd(2)–Cl(3)	230.5(9)	O(1)–H(2O1)···Cl(2)	174.4(3)
Pd(3)–Cl(4)	230.4(9)	O(1)–H(1O1)···Cl(6)	174.6(3)
Pd(3)–Cl(5)	236.1(9)	O(2)–H(2O2)···Cl(3)	175.0(2)
Pd(4)–Cl(6)	231.6(9)	O(2)–H(1O2)···Cl(5)	175.1(2)
Pd(2)–O(1)	210.2(3)		
Pd(4)–O(2)	212.3(3)		

The reaction of **17** and $[PtI_2(cod)]$ was carried out at high temperature (toluene reflux, 24 h). After repeated crystallisations, dark orange crystals of the already described compound **20** and violet crystals of $[\{NiI(\mu\text{-}S\text{-}SC_6H_4\text{-}2\text{-}PPh_2)\text{-}\kappa^2S,P\}_2]$ (**22**) could be separated. In **22** the cleavage of the $AsPh_2$ groups has occured, which could be due to the applied high temperature reaction conditions. **22** crystallises in the triclinic space group $P\bar{1}$ with two molecules in the unit cell. The molecular structure of **22** is depicted in Figure 43. A selection of bond lengths and angles is listed in Table 21. The dinuclear structure consists of two nickel–phosphanylthiolato units joined together by two sulfur bridges between the two metal centres. The environment around both metal centres is square planar and each nickel is coordinated by a terminal iodo ligand as well. The experimental Ni···Ni distances in **22** are longer than the limit of the sum of the covalent radii of two nickel atoms, i.e. 248 pm, indicateing an absence of a direct metal–metal bond.

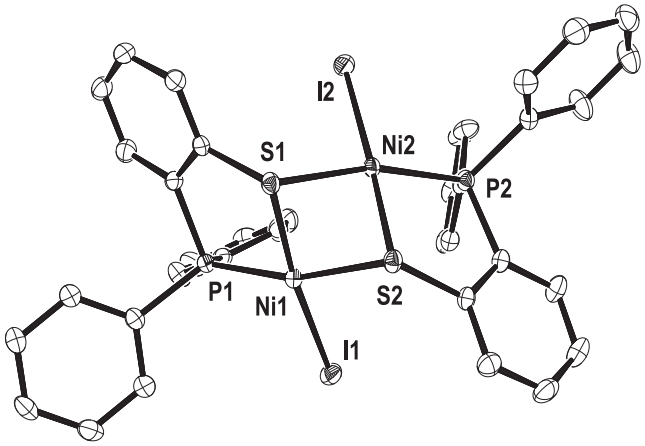

Figure 43. Molecular structure of [{NiI(μ-*S*-SC_6H_4-2-PPh_2)-κ^2*S,P*}$_2$] (**22**). Hydrogen atoms are omitted for clarity.

Table 21. Selected bond lengths and angles for **22.**

Bond lengths [pm]				Bond angles [°]	
Ni(1)–P(1)	216.8(6)	Ni(2)–P(2)	215.9(6)	P(1)–Ni(1)–S(2)	165.1(2)
Ni(1)–S(1)	217.2(6)	Ni(2)–S(1)	226.6(6)	S(1)–Ni(1)–I(1)	177.0(2)
Ni(1)–S(2)	226. 8(6)	Ni(2)–S(2)	219.7(6)	P(2)–Ni(2)–S(1)	163.3(2)
Ni(1)–I(1)	248.7(3)	Ni(2)–I(2)	249.4(3)	S(2)–Ni(2)–I(2)	173.4(2)
Ni(1)–Ni(2)	268.3(4)				

7. General conclusions

The first part of the original contributions (chapter 3) is concerned with the synthesis and characterisation of the new heterotopic ligands containing As/P, As/S/P and As/S/As as donor atoms: 1-PPh_2-2-$S(AsPh_2)C_6H_4$ (**1**), 1-$AsPh_2$-2-$S(PPh_2)C_6H_4$ (**2**), 1-PPh_2-2-$S(C_4H_9)$-3-$AsPh_2$-C_6H_3 (**3**, **SPAs**), 1,3-$AsPh_2$-2-$S(C_4H_9)C_6H_3$ (**4**, **SAs2**) and 1-PPh_2-2-SH-3-$AsPh_2$-C_6H_3 (**5**, **SHPAs**). The synthesis of **4** required the preparation of 1-$AsPh_2$-2-$S(C_4H_9)C_6H_4$ (**4a**) as precursor, which proved to be a novel compound as well.

The compounds were characterised by NMR, IR spectroscopy, mass spectrometry, elemental analysis and X-ray structure analysis (in case of **1**, **3**–**5**).

Furthermore, this thesis describes the coordinative properties of **1** toward group 10 metal dihalides (chapter 4.1) and metal carbonyl complexes of Mo, Mn and Fe (chapter 4.2). The metal-mediated cleavage of the As–S bond of the ligand, respectively the role of the neighbouring PPh_2 group in the coordination to metal centres was studied. All reactions of **1** with transition metal complexes featured the cleavage of the As–S bond and coordination of the resulting phosphanylthiolato ligand $(SC_6H_4\text{-}2\text{-}PPh_2)^-$. The results are summarised in the following:

- Reactions with $[MX_2(cod)]$ (M = Pd, X = Cl; M = Pt, X = I) led to trinuclear complexes $[(cis\text{-}M\{(\mu\text{-}S\text{-}SC_6H_4\text{-}2\text{-}PPh_2)\text{-}\kappa^2S,P\}_2)\text{-}MX_2\text{-}MX\{(\mu\text{-}S\text{-}SC_6H_4\text{-}2\text{-}PPh_2)\text{-}\kappa^2S,P\}]$ [M = Pd, X = Cl (**8**); M = Pt, X = I (**10**)] as kinetic products, followed by formation of the thermodynamic products $[PtI\{(\mu\text{-}S\text{-}SC_6H_4\text{-}2\text{-}PPh_2)\text{-}\kappa^2S,P\}]_3$ (M = Pd, X = Cl (**7**); M = Pt, X = I (**9**)). The isomerisation process was followed by $^{31}P\{^1H\}$ NMR spectroscopy; all of the structural isomers were isolated and characterised by X-ray structure analysis. In contrast, the reaction of **1** with $NiCl_2\cdot 6H_2O$ led only to the bischelate complex *trans*-$[Ni\{(SC_6H_4\text{-}2\text{-}PPh_2)\text{-}\kappa^2S,P\}_2]$ (**6**).
- Reactions of **1** with $[MoCp(CO)_3]_2$ and $[FeCp(CO)_2]_2$ lead to $[MoCp(CO)_2\{(SC_6H_4\text{-}2\text{-}PPh_2)\text{-}\kappa S,P\}]$ (**11**) and $[FeCp(CO)\{(SC_6H_4\text{-}2\text{-}PPh_2)\text{-}\kappa S,P\}]$ (**15**). Not only has the As–S bond of **1** been cleaved, but also the disaggregation of the initial dimeric metal complexes through the scission of the metal-metal bonds was observed.
- Reaction of **1** with $[Mn_2(CO)_{10}]$ led to two metal complexes. $[Mn_2(CO)_7(\mu\text{-}AsPh_2)\{(SC_6H_4\text{-}2\text{-}PPh_2)\text{-}\kappa S,P\}]$ (**12**) is the only reaction product with **1** which contains all three donor atoms in its structure. The cleaved $AsPh_2$ group is included in the final complex and bridges two Mn atoms, while the P,S chelating pocket coordinates to one Mn centre. At the same time $[Mn_2(CO)_8(\mu\text{-}AsPh_2)_2]$ (**13**) serves as the single example where the metal centres are coordinated only by bridging $AsPh_2$ groups and the $(SC_6H_4\text{-}2\text{-}PPh_2)^-$ part of the ligand is excluded.

- The complex $[Fe(CO)_2\{(SC_6H_4\text{-}2\text{-}PPh_2)\text{-}\kappa^2S,P)\}_2]$ (**14**) is a good example that ligands containing mixed-donor P,S chelating pockets tend to form mononuclear complexes of the general formula $M(P,S)_2$.

Chapter 5 describes the coordination chemistry of **SPAs** with rhodium and group 10 metal(II) halides. Due to the two flanking tertiary E donor groups (E = As, P) in the *ortho*-positions, in some cases sulfur-bridged trimetallic complexes ($[RhCl_2\{(Rh(cod)(SC_6H_3\text{-}2\text{-}PPh_2\text{-}3\text{-}AsPh_2)\text{-}\kappa S,P)\text{-}\kappa S,As\}_2][RhCl_2(cod)]$ (**16**), $[Pt\{(PtI_2(SC_6H_3\text{-}2\text{-}PPh_2\text{-}3\text{-}AsPh_2)\text{-}\kappa S,P)\text{-}\kappa S,As\}_2]$ (**20**)) and bimetallic complexes ($[\{Pd_2Cl_2(SC_6H_3\text{-}2\text{-}PPh_2\text{-}3\text{-}AsPh_2)\}_2(\mu\text{-}Cl)_2]$ (**18**) were formed. However, regardless of the tridentate structural motif of **SPAs**, reactions with $NiCl_2{\cdot}6H_2O$ led exclusively to *trans*-$[Ni\{(SC_6H_3\text{-}2\text{-}PPh_2\text{-}3\text{-}AsPh_2)\text{-}\kappa^2S,P\}_2]$ (**17**), while the 2:1 reactions with $[PtI_2(cod)]$ led to the mononuclear complex *cis*-$[Pt\{(SC_6H_3\text{-}2\text{-}PPh_2\text{-}3\text{-}AsPh_2)\text{-}\kappa^2S,P\}_2]$ (**19a**). The two trinuclear species **16** and **20** have $Rh(As,S)_2$ and $Pt(As,S)_2$ moieties, respectively, as central units, while each terminal metal centre is chelated by the P,S donor groups. In the mononuclear complexes mentioned above, two ligands coordinate to the metal centre through their P,S chelating compartments in a *trans* (**17**) or in a *cis* (**19a**) arrangement, leaving the two $AsPh_2$ groups still free for further coordination. Theoretical calculations on **SPAs** and **SHPAs** predicted, that the P,S chelating pocket will be favoured over the As,S unit during an electrophilic attack. This has been evidenced experimentally in mononuclear complexes of **SPAs**, namely **17** and **19a**. Furthermore, computational studies of the *cis*-*trans* isomerism of **17** and **19a** showed that the *trans* isomer is energetically always more favoured than the *cis* forms. This clearly explains why for the nickel compounds only the *trans* isomer (**17**) was observed experimentally. For the platinum analogues, the possibility of intramolecular π-π interactions still favours the formation of the corresponding *cis* isomer (**19a**), albeit the weaker nature of these π-π interactions between the phenyl rings of two **SPAs** moieties relative to the π-π interactions between the phenyl rings of two **BiphPS** moieties.[94] Compound **18** is constructed from two dinuclear systems which are held together through chloro bridges. Each chelating compartment of the ligand is coordinating to one

palladium atom, and the metal centres are brought close to each other through the bridging sulfur atom.

Since the structure of **17** still offers two free $AsPh_2$ groups in *trans* arrangement for further coordination, its subsequent reaction with group 10 metal(II) halides was investigated (chapter 6). The reaction with $NiCl_2{\cdot}6H_2O$ did not take place, not even at elevated temperatures (>110 °C). In order to try to synthesise bimetallic trinuclear complexes, the reaction of **17** with $[PdCl_2(cod)]$ and $[PtI_2(cod)]$ was carried out. However, none of the obtained complexes proved to be a bimetallic species. The structure of $[\{Pd_2Cl_2(OH_2)(SC_6H_3\text{-}2\text{-}PPh_2\text{-}3\text{-}AsPh_2)\}_2]$ (**21**) lacks the presence of the Ni centre, the chelating compartments being occupied by two palladium atoms, and the complex is constructed from two dinuclear systems held together by two intermolecular hydrogen bonds (OH···Cl). Reaction of **17** and $[PtI_2(cod)]$ resulted in the previously described compound **20** and in $[\{NiI(\mu\text{-}S\text{-}SC_6H_4\text{-}2\text{-}PPh_2)\text{-}\kappa^2S,P\}_2]$ (**22**). While in compound **20**, the Ni atom is excluded from the structure, complex **22** has two Ni centres and a dimeric structure with a bent Ni_2S_2 central unit. The driving force for bending in **22** was clearly identified as the $d \rightarrow p^*$ donor–acceptor interactions between the two nickel atoms. At the same time **22** shows cleavage of the $AsPh_2$ groups, thus, the metal centres are coordinated by two $(SC_6H_4\text{-}2\text{-}PPh_2)^-$ moieties and two iodo ligands. Scission of the C–As bond is assumed to occur due to the high temperature reaction conditions. The reasons for the exchange of nickel during the reaction of **17** with $[PdCl_2(cod)]$ or $[PtI_2(cod)]$ is not clear. The smaller atomic radius of nickel in comparison to that of platinum and palladium and the lower affinity of nickel(II) for the phosphorus centre in comparison to palladium(II) and platinum(II) could be the cause of the occurring Ni/Pd and Ni/Pt substitution, but in order to understand the mechanism of the reaction, further studies are needed.

References

1. P. Braunstein, F. Naud, *Angew. Chem. Int. Ed.,* **2001**, *40*, 680; P. Braunstein, F. Naud, *Angew. Chem.,* **2001**, *113*, 702.
2. C. S. Slone, D. A. Weinberger, C. A. Mirkin, *Prog. Inorg. Chem.,* **1999**, *48*, 233.
3. M. Bassetti, *Eur. J. Inorg. Chem.*, **2006**, 4473.
4. A. Bader, E. Linder, *Coord. Chem. Rev.*, **1991**, *108*, 27.
5. J. R. Dilworth, N. Wheatley, *Coord. Chem. Rev.*, **2000**, *199*, 89.
6. J. J. Schneider, *Nachr. Chem.*, **2000**, *48*, 614.
7. J. J. Schneider, *Nachr. Chem.,* **2000**, *48*, 618.
8. K. N. Gavrilov, A. I. Polosukhin, *Russ. Chem. Rev.*, **2000**, *69*, 661.
9. G. Delapierre, G. Buono, *Actualite Chimique*, **2003**, *2*, 3.
10. J. C. Jeffrey, T. B. Rauchfuss, *Inorg. Chem.,* **1979**, *18*, 2658.
11. P. Braunstein, D. Matt, F. Mathey, D. Thavard, *J. Chem. Res. Synop.*, **1978**, 232.
12. P. Braunstein, D. Matt, F. Mathey, D. Thavard, *J. Chem. Res. Miniprint*, **1978**, 3041.
13. P. Braunstein, *J. Organomet. Chem*., **2004**, *689*, 3953.
14. J. S. Kingsbury, J. P. A. Harrity, P. J. Bonitatebus, A. H. Hoveyda, *J. Am. Chem. Soc.*, **1999**, *121*, 791.
15. S. B. Garber, J. S. Kingsbury, B. L. Gray, A. H. Hoveyda, *J. Am. Chem. Soc*., **2000**, *122*, 868.
16. H. Fritzsche, U. Hasserodt, F. Korte, *Angew. Chem. Int. Ed.*, **1964**, *3*, 64; H. Fritzsche, U. Hasserodt, F. Korte, *Angew. Chem.*, **1963**, *75*, 1205.
17. R. Fusco, C. A. Peri, V. Corradini, Montecatini, *Patent*, **1963**, BE621008.
18. R. A. N. McLean, *Inorg. Nucl. Chem. Letters*, **1969**, *5*, 745.
19. S. C. Peake, R. Schmutzler, *J. Chem. Soc. A, Inorg. Phys. Theor.*, **1970**, 1049.
20. L. Horner, J. Manfred, *Phosphorus and Sulfur*, **1980**, *8*, 215.
21. C. D. Hall, B. R. Tweedy, R. Kayhanian, J. R. Lloyd, *J. Chem. Soc., Perkin Trans. 2,* **1992**, 775.
22. V. Cadierno, M. Zablocka, B. Donnadieu, A. Igau, J.-P. Majoral, A. Skowronska, *Chem. Eur. J*., **2001**, *7*, 221.
23. L.-B. Han, T. D. Tilley, *J. Am. Chem. Soc*., **2006**, *128*, 13698.
24. T. D. Sideris, P. V. Ioannou, *Phosphorus, Sulfur, and Silicon*, **2006**, *181*, 751.
25. B. E. Job, R. A. N. McLean, D. T. Thompson, *Chem. Commun*., **1966**, 895.
26. G. Le Borgne, R. Mathieu, *J. Organomet. Chem.*, **1981**, *208*, 201.
27. G. Conole, J. E. Davies, J. D. King, M. J. Mays, M. McPartlin, H. R. Powell, P. R. Raithby, *J. Organomet. Chem*., **1999**, *585*, 141.
28. A. J. Edwards, A. Martin, M. J. Mays, P. R. Raithby, G. A. Solan, *J. Chem. Soc., Chem. Commun*., **1992**, 1416.
29. G. Conole, M. Kessler, M. J. Mays, G. E. Pateman, G. A. Solan, *Polyhedron*, **1998**, *17*, 2993.
30. A. J. Edwards, A. Martin, M. J. Mays, D. Nazar, P. R. Raithby, G. A. Solan, *J. Chem. Soc., Dalton Trans*., **1993**, 355.

31. A. Martin, M. J. Mays, P. R. Raithby, G. A. Solan, *J. Chem. Soc., Dalton Trans*., **1993**, 1431.
32. S. L. Ingham, M. J. Mays, P. R. Raithby, G. A. Solan, B. V. Sundavadra, G. Conole, M. Kessler, *J. Chem. Soc., Dalton Trans*., **1994**, 3607.
33. J. D. King, M. J. Mays, G. E. Pateman, P. R. Raithby, M. A. Rennie, G. A. Solan, N. Choi, G. Conole, M. McPartlin, *J. Chem. Soc., Dalton Trans*., **1999**, 4447.
34. E. Block, G. Ofori-Okai, J. Zubieta, *J. Am. Chem. Soc.,* **1989**, *111*, 2327.
35. A. Hildebrand, *PhD Thesis*, Universität Leipzig, **2006**.
36. A. Hildebrand, P. Lönnecke, L. Silaghi-Dumitrescu, E. Hey-Hawkins, *J. Chem. Soc., Dalton Trans.*, **2008**, 4639.
37. S. E. Livingstone, T. N. Lockyer, *Inorg. Nucl. Chem. Lett.*, **1967**, *3*, 35.
38. G. D. Figuly, C. K. Loop, J. C. Martin, *J. Am. Chem. Soc.*, **1989**, *111*, 654.
39. E. Block, V. Eswarakrishnan, M. Gernon, G. Ofori-Okai, C. Saha, K. Tang, J. Zubieta*, J. Am. Chem. Soc.*, **1989**, *111*, 658.
40. K. Smith, C. M. Lindsay, G. J. Pritchard, *J. Am. Chem. Soc.*, **1989**, *111***,** 665.
41. B. J. Wakefield, in *The Chemistry of Organolithium Compounds*, Pergamon, Oxford, UK, **1974**.
42. M. Gray, M. Tinkl, V. Sniekus, in *Comprehensive Organometallic Chemistry II*, G. Wilkinson, F. G. A. Stone, E. Abel, Eds., Pergamon, Oxford, UK, **1991**, vol. 1, ch. 1.
43. Jr. A. Streitwieser, *Acc. Chem. Res*., **1984**, *17*, 353.
44. D. Kost, J. Klein, Jr. A. Streitwieser, G. W. Schriver, *Proc. Natl. Acad. Sci*. *U.S.A*., **1982**, *79*, 3922.
45. E. Block, H. Kang, G. Ofori-Okai, J. Zubieta, *Inorg. Chim. Acta*, **1989**, *166*, 155.
46. J. R. Dilworth, J. R. Miller, N. Wheatley, M. J. Baker, J. G. Sunley, *J. Chem. Soc., Chem. Commun.*, **1995**, 1579.
47. A. Hildebrand, M. B. Sárosi, P. Lönnecke, L. Silaghi-Dumitrescu, E. Hey-Hawkins, *Rev. Roum. Chim.,* **2010**, *55*, 885.
48. A. Benefiel, D. M. Roundhill, W. C. Fultz, A. L. Rheingold, *Inorg. Chem.,* **1984**, *23*, 3316.
49. J. Real, E. Prat, A. Polo, A. Álvarez-Larena, J. F. Piniella, *Inorg. Chem. Commun.,* **2000**, *3*, 221.
50. D. Canseco-González, V. Gómez-Benitez, S. Hernández-Ortega, R. A. Toscano, D. Morales-Morales, *J. Organomet. Chem.,* **2003**, *679*, 101.
51. J. Fierro-Arias, D. Morales-Morales, S. Hernández-Ortega*, Acta Cryst. E,* **2008**, *64*, m1196.
52. A. Benefiel, D. M. Roundhill, *Inorg. Chem.,* **1986**, *25*, 4027.
53. J. R. Dilworth, A. J. Hutson, J. Zubieta, Q. Chen, *Trans. Met. Chem.,* **1994**, *19*, 61.
54. J. S. Kim, J. H. Reibenspies, M. Y. Darensbourg, *J. Am. Chem. Soc*. **1996**, *118*, 4115.
55. E. Block, G. Ofori-Okai, H. Kang, J. Zubieta, *Inorg. Chim. Acta,* **1991**, *188*, 7.
56. A. Hildebrand, I. Sárosi, P. Lönnecke, L. Silaghi-Dumitrescu, Menyhárt B. Sárosi, I. Silaghi-Dumitrescu, E. Hey-Hawkins, *Inorg. Chem.*, **2012**, submitted.
57. J. R. Dilworth, Y. Zheng, D. V. Griffiths, *J. Chem. Soc., Dalton Trans*., **1999**, 1877.

58. A. Beganskiene, L. R. Pignotti, V. Baltramiejunaite, R. L. Luck, E. Urnezius, *Inorg. Chim. Acta*, **2008**, *361*, 1349.
59. C. Zhu, N. Yukimura, M. Yamane, *Organometallics*, **2010**, *29*, 2098.
60. E. Nakamura, N. Yoshikai, M. Yamanaka, *J. Am. Chem. Soc*., **2002**, *124*, 7181.
61. Y. Nishibayashi, M. D. Milton, Y. Inada, M. Yoshikawa, I. Wakiji, M. Hidai, S. Uemura, *Chem. Eur. J*., **2005**, *11*, 1433.
62. J. Mason, *Multinuclear NMR*, Plenum Press, New York, USA, **1987**.
63. S. B. Wild, *The Chemistry of Organic Arsenic, Antimony and Bismuth Compounds,* S. Patai Ed.; John Wiley & Sons Ltd.: Chichester, **1994**.
64. F. F. Blicke, F.D. Smith, *J .Chem. Soc.,* **1929**, *51*, 1558.
65. R. D. Gigauri, G. N. Chachava, B. D. Chernokal'skii, M. M. Ugulava, *Z. Obsc. Chim*., **1972**, *42*, 1537.
66. A. L. Mackay, *Acta Cryst*. *A*, **1984**, *40*, 165.
67. P. Suomalainen, S. Jääskeläinen, M. Haukka, R. H. Laitinen, J. Pursiainen, T. A. Pakkanen, *Eur. J. Inorg. Chem.,* **2000**, 2607.
68. K. Tani, S. Hanabusa, S. Kato, S. Mutoh, S. Suzuki, M. Ishida, *J. Chem. Soc., Dalton Trans.,* **2001**, 518.
69. P. Perez-Lourido, J. A. Garcia-Vasquez, J. Romero, A. Sousa, E. Block, K. P. Maresca, J. Zubieta, *Inorg. Chem.,* **1999**, *38*, 538.
70. R. H. Laitinen, H. Riihimaki, M. Haukka, S. Jaaskelainen, T. A. Pakkanen, J. Pursiainen, *Eur. J. Inorg. Chem.*, **1999**, 1253.
71. A. P. West Junior, N. Smyth, C. M. Krami, D. M. Ho, R. A. Pascal Junior, *J. Org. Chem.,* **1993**, *58*, 3502.
72. J. I. van der Vlugt, J. M. Bonet, A. M. Millis, A. L. Spek, D. Vogt, *Tetrahedron Lett.,* **2003**, *44*, 4389.
73. W. Goerz, D. Vogt, U. Englert, M. D. K. Boele, L. A. van der Veen, P. C. J. Kamer, P. W. N. M. van Leeuwen, *J. Chem. Soc., Dalton Trans.,* **1998**, 2981.
74. C. Bauduin, E. B. Kaloun, C. Darcel, S. Juge, *J. Org. Chem.,* **2003**, *68*, 4293.
75. A. Pintado-Alba, H. de la Riva, M. Nieuwhuyzen, D. Bautista, P. R. Raithby, H. A. Sparkes, S. J. Teat, J. M. Lopez-de-Luzuriaga, M. C. Lagunas, *J. Chem. Soc., Dalton Trans.,* **2004**, 3459.
76. D. W. Allen, J. C. Coppola, O. Kennard, F. G. Mann, W. D. S Motherwell, D. G. Watson, *J. Chem. Soc. C,* **1970**, 810.
77. R. Bally, *Acta Cryst.,* **1967**, *23*, 295.
78. P. H. Javora, R. A. Zingaro, E. A. Meyers, *Cryst. Struct. Commun.,* **1975**, *4*, 67.
79. G. C. Pappalardo, *Acta Cryst. C,* **1983**, *39*, 1618.
80. H. Gilman, F. J. Webb, *J. Am. Chem. Soc*., **1940**, *62*, 987.
81. H. Gilman, F. J. Webb, *J. Am. Chem. Soc*., **1949**, *71*, 4062.
82. M. Micha-Screttas, C. G. Screttas, J. *Org. Chem*., **1977**, *42*, 1462.
83. L. Horner, A. J. Lawson, G. Simons, *Phosphorus and Sulfur*, **1982**, *12*, 353.
84. T.-S. Chou, C.-H. Tsao, S. C. Hung, *J. Organomet. Chem*., **1986**, *312*, 53.
85. I. Sárosi, A. Hildebrand, P. Lönnecke, L. Silaghi-Dumitrescu, E. Hey-Hawkins, *Dalton Trans.*, **2012**, DOI:10.1039/C2DT12506D.
86. R. M. Bozorth, *J. Am. Chem. Soc*., **1923**, *45*, 1621.
87. J. Kopf, K. von Deuten, G. Klar, *Inorg. Chim. Acta*, **1980**, *37*, 67.

88. B. J. McKerley, K. Reinhardt, J. L. Mills, G. M. Reisner, J. D.Kopf, I. Bernal, *Inorg. Chem. Acta*, **1978**, *31*, L411.
89. I. Bernal, H. Brunner, W. Meier, H. Pfisterer, J. Wachter, M. L. Ziegler, *Angew. Chem. Int. Ed.*, **1984**, *23*, 438; I. Bernal, H. Brunner, W. Meier, H. Pfisterer, J. Wachter, M. L. Ziegler, *Angew. Chem.*, **1984**, *96*, 428.
90. H. Brunner, H. Kauermann, B. Nuber, J. Wachter, M. L. Ziegler, *Angew. Chem. Int. Ed.*, **1986**, *25*, 557; H. Brunner, H. Kauermann, B. Nuber, J. Wachter, M. L. Ziegler, *Angew. Chem.*, **1986**, *98*, 551.
91. H. Brunner, B. Nuber, L. Poll, J. Wachter, *Angew. Chem. Int. Ed.*, **1993**, *32*, 1627; H. Brunner, B. Nuber, L. Poll, J. Wachter, *Angew. Chem.*, **1993**, *105*, 1699.
92. H. Brunner, L. Poll, J. Wachter, *J. Organomet. Chem*., **1994**, *471*, 117.
93. H. Brunner, L. Poll, J. Wachter, *Polyhedron*, **1996**, *15*, 573.
94. H. Brunner, H. Kauermann, L. Poll, B. Nuber, J. Wachter, *Chem. Ber*., **1996**, *129*, 657.
95. A. Hildebrand, I. Sárosi, P. Lönnecke, L. Silaghi-Dumitrescu, Menyhárt B. Sárosi, I. Silaghi-Dumitrescu, E. Hey-Hawkins, *Dalton Trans.*, **2012**, submitted.
96. D. Sellmann, D. Häußinger, F. W. Heinemann, *Eur. J. Inorg. Chem*., **1999**, 1715.
97. C. A. Ghilardi, S. Midollini, A. Orlandini, G. Scapacci, A. Vacca, *J. Organomet. Chem*., **1993**, *461*, C4.
98. J. H. Chou, M. G. Kanatzidis, *Inorg. Chem*., **1994**, *33*, 5372.
99. Y. Y. Davidson, S. Ch. Chang, R. E. Norman, *J. Chem. Soc., Dalton Trans*., **1995**, 77.
100. M. Capdevila, W. Clegg, P. Gonzáles-Duarte, I. Mira, *J. Chem. Soc., Dalton Trans.,* **1992**, 173.
101. G. A. Barclay, E. M. McPartlin, N. C. Stephenson, *Inorg. Nucl. Chem. Letters,* **1967**, *3*, 397.
102. E. M. McPartlin, N. C. Stephenson, *Acta Cryst. B,* **1969**, *25*, 1659.
103. D. Sellmann, F. Geipel, F. W. Heinemann, *Eur. J. Inorg. Chem.,* **2000**, 271.
104. Z. Zhu, T. Kajino, M. Kojima, K. Nakajima, *Inorg. Chim. Acta,* **2003**, *355*, 197.
105. L. Adrio, J. M. Antelo, J. J. Fernández, K. K. (M.) Hii, M. T. Pereira, J. M. Vila, *J. Organomet. Chem*., **2009**, *694*, 747.
106. H. Adams, N. A. Bailey, A. N. Day, M. J. Morris, M. M. Harrison, *J. Organomet. Chem*., **1991**, *407*, 247.
107. R. F. Lambert, *Chem. Ind*. (London), **1961**, 830.
108. H. Ashton, B. Brady, A. R. Manning, *J. Organomet. Chem.,* **1981**, *221*, 71.
109. S. Hayashida, T. Kawamura, T. Yonezawa, *Chem. Soc. Jpn*., *Chem. Lett*., **1981**, 985.
110. T. Kawamura, S. Enoki, S. Hayashida, T. Yonezawa, *Bull. Chem. Soc. Jpn*., **1982**, *55*, 3417.
111. N. Chaozhou, Z. Zhiming, X. Zuowei, Q. Changtao, H. Yaozeng, *Jiegou Huaxue (Chin. J. Struct. Chem.*), **1986**, *5*, 181.
112. J. D. Franolic, M. Millar, S. A. Koch, *Inorg. Chem.,* **1995**, *34*, 1981.
113. H.-F. Hsu, S.A. Koch, *J. Am. Chem. Soc.,* **1997**, *119*, 8371.
114. E. A. Laifa, N. Benali-Cherif, *Acta Cryst. E,* **2003**, *59*, m283
115. J. Takács, L. Markó, L. Párkányi, *J. Organom. Chem.,* **1989**, *361*, 109.
116. M. M. Van Dyk, P. H. Van Rooyen, S. Lotz, *Inorg. Chim. Acta,* **1989**, *163*, 167.

117. O. Baldovino-Pantaleón, G. Ríos-Moreno, R. A. Toscano, D. Morales-Morales, *J. Organomet. Chem.,* **2005**, *690*, 2880.
118. G. Hogarth, M. O'Brien, D. A. Tocher, *J. Organomet. Chem.,* **2003**, *672*, 29.
119. P. Pérez-Lourido, J. Romero, J.A. García-Vázquez, J. Castro, A. Sousa, L. Cooper, J. R. Dilworth, R.L. Richards, Y. Zheng, J.A. Zubieta, *Inorg. Chim. Acta,* **2003**, *356*, 193.
120. A. M. Vălean, *PhD Thesis*, "Babes-Bolyai" University, **2008**.
121. R. Atencio, M. A. Casado, M. A. Ciriano, F. J. Lahoz, J. J. Perez-Torrente, A. Tiripicchio, L. A. Oro, *J. Organomet. Chem.*, **1996**, *514*, 103.
122. T. Iwasa, H. Shimada, A. Takami, H. Matsuzaka, Y. Ishii, M. Hidai, *Inorg. Chem.*, **1999**, *38*, 2851.
123. J. A. Camerano, M. A. Casado, M. A. Ciriano, F. J. Lahoz, L. A. Oro, *Organometallics*, **2005**, *24*, 5147.
124. P. G. Eller, J. M. Riker, D. W. Meek, *J. Am. Chem. Soc*., **1973**, *95*, 3540.
125. P. Perez-Lourido, J. Romero, J. A. Garcia-Vazquez, A. Sousa, J. Zubieta, K. Maresca, *Polyhedron*, **1998**, *17*, 4457.
126. C. Kluwe, J. A. Davies, *Organometallics*, **1995**, *14*, 4257.
127. J. P. Beale, N. C. Stephenson, *Acta Cryst. B,* **1971**, *27*, 73.
128. R. Poli, J. N. Harvey, *Chem. Soc. Rev.*, **2003**, *32*, 1.
129. A search in the CCDC database (December 2011) for OH···Cl hydrogen bonds gives 60 OH···Cl distances in the 187.4 and 229.3 pm range (mean: 217.7 pm, median: 220.9 pm).
130. A. E. Reed, L. A. Curtiss, F. Weinhold, *Chem. Rev.*, **1988**, *88*, 899.
131. P. Pérez-Lourido, J. Romero, J. A. García-Vázquez, A. Sousa, J. Zubieta, K. Maresca, *Polyhedron*, **1988**, *17*, 4457.
132. E. Block, G. Ofori-Okai, H. Kang, J. Zubieta, *Inorg. Chim. Acta* **1991**, *188*, 7.
133. P. Fernández, A. Sousa-Pedrares, J. Romero, M. L. Durán, A. Sousa, P. Pérez-Lourido, J. A. García-Vázquez, *Eur. J. Inorg. Chem*., **2010**, 814
134. F. A. Cotton, M. Matusz, R. Poly, X. Feng, *J. Am. Chem. Soc.* **1988**, *110*, 1144.
135. E. Erkizia, R. R. Conry, *Inorg. Chem.* **2000**, *39*, 1674 and references therein.
136. G. Aullón, P. Alemany, S. Alvarez, *Inorg. Chem*., **1996**, *35*, 5061.
137. G. Aullón, G. Ujaque, A. Lledós, S. Alvarez, P. Alemany, *Inorg. Chem*., **1998**, *37*, 804.
138. K. B. Wiberg, *Tetrahedron*, **1968**, *24*, 1083.
139. G. Giordano, R. H. Crabtree, in *Reagents for Transition Metal Complex and Organometallic Synthesis, Inorg. Synth*., R. J. Angelici, Ed., Wiley and Sons, New York, **1990**, vol. 28, ch. 2.
140. D. Drew, J. R. Doyle, in *Inorg. Synth*., A. Cotton, Ed., McGraw-Hill, Inc., New York, **1972**, vol. 13, ch. 2.
141. G. Bauer, *Handbuch der Präparativen Anorganische Chemie*, Band III, Ferdinand Enke Verlag, Stuttgart, **1981**.
142. CrysAlisPro: Data collection and data reduction software package, Agilent Technologies; SCALE3 ABSPACK: Empirical absorption correction using spherical harmonics.

143. SHELX includes SHELXS-97, SHELXL-97: G. M. Sheldrick, *Acta Cryst. A*, **2008**, *64*, 112; SIR92 – A program for crystal structure solution, A. Altomare, G. Cascarano, C. Giacovazzo, A. Guagliardi, *J. Appl. Crystallogr.*, **1993**, *26*, 343.
144. ORTEP3 for Windows: L. J. Farrugia, *J. Appl. Cryst*., **1997**, *30*, 565.
145. GaussView, Version 4.1, Semichem Inc., **2000-2006**.
146. M. J. Frisch, G. W. Trucks, H. B. Schlegel, G. E. Scuseria, M. A. Robb, J. R. Cheeseman, G. Scalmani, V. Barone, B. Mennucci, G. A. Petersson, H. Nakatsuji, M. Caricato, X. Li, H. P. Hratchian, A. F. Izmaylov, J. Bloino, G. Zheng, J. L. Sonnenberg, M. Hada, M. Ehara, K. Toyota, R. Fukuda, J. Hasegawa, M. Ishida, T. Nakajima, Y. Honda, O. Kitao, H. Nakai, T. Vreven, J. Montgomery, J. A. , J. E. Peralta, F. Ogliaro, M. Bearpark, J. J. Heyd, E. Brothers, K. N. Kudin, V. N. Staroverov, R. Kobayashi, J. Normand, K. Raghavachari, A. Rendell, J. C. Burant, S. S. Iyengar, J. Tomasi, M. Cossi, N. Rega, J. M. Millam, M. Klene, J. E. Knox, J. B. Cross, V. Bakken, C. Adamo, J. Jaramillo, R. Gomperts, R. E. Stratmann, O. Yazyev, A. J. Austin, R. Cammi, C. Pomelli, J. W. Ochterski, R. L. Martin, K. Morokuma, V. G. Zakrzewski, G. A. Voth, P. Salvador, J. J. Dannenberg, S. Dapprich, A. D. Daniels, O. Farkas, J. B. Foresman, J. V. Ortiz, J. Cioslowski, D. J. Fox, *Gaussian 09, Revision A.02*, Gaussian, Inc., Wallingford CT, **2009**.
147. D. Feller, *J. Comput. Chem.*, **1996**, *17*, 1571.
148. K. L. Schuchardt, B. T. Didier, T. Elsethagen, L. Sun, V. Gurumoorthi, J. Chase, J. Li, T. L. Windus, *J. Chem. Inf. Model.*, **2007**, *47*, 1045.
149. J. Tomasi, B. Mennucci, R. Cammi, *Chem. Rev.*, **2005**, *105*, 2999.
150. A. D. Becke, *J. Chem. Phys.*, **1993**, *98*, 5648.
151. C. Lee, W. Yang, R. G. Parr, *Phys. Rev. B*, **1988**, *37*, 785.
152. R. Ditchfield, W. Hehre, J. A. Pople, *J. Chem. Phys.*, **1971**, *54*, 724.
153. P. J. Hay, W. R. Wadt, *J. Chem. Phys.*, **1985**, *82*, 270.
154. P. J. Hay, W. R. Wadt, *J. Chem. Phys.*, **1985**, *82*, 284.
155. P. J. Hay, W. R. Wadt, *J. Chem. Phys.*, **1985**, *82*, 299.
156. T. H. Dunning Jr., P. J. Hay, in *Modern Theoretical Chemistry*, H. F. Schaefer III, Ed., Plenum, New York, **1976**, vol. 3, p. 1-28.
157. Y. Zhao, D. G. Truhlar, *Theor. Chem. Acc.*, **2008**, *120*, 215.
158. Y. Zhao, D. G. Truhlar, *Acc. Chem. Res.,* **2008**, *41*, 157.
159. P.J. Hay, W.R. Wadt, *J. Chem. Phys.*, **1985**, *82*, 299.
160. A.W. Ehlers, M. Bohme, S. Dapprich, A. Gobbi, A. Hollwarth, V. Jonas, K.F. Kohler, R. Stegmann, A. Veldkamp, G. Frenking, *Chem. Phys. Lett.*, **1993**, *208*, 111.
161. C.E. Check, T.O. Faust, J.M. Bailey, B.J. Wright, T.M. Gilbert, L.S. Sunderlin, *J Phys. Chem. A*, **2001**, *105*, 8111.
162. L.E. Roy, P.J. Hay, R.L. Martin, *J. Chem. Theory Comput.*, **2008**, *4*, 1029.

Acknowledgements

The financial support provided from the following sources is gratefully acknowledged:

Investing in people! PhD scholarship, Project co-financed by the
SECTORAL OPERATIONAL PROGRAMME HUMAN RESOURCES
DEVELOPMENT 2007-2013
Priority Axis 1 "Education and training in support for growth and development of a knowledge based society"
Key area of intervention 1.5: Doctoral and post-doctoral programmes in support of research.
Contract **POSDRU 6/1.5/S/3** – „DOCTORAL STUDIES: THROUGH SCIENCE TOWARDS SOCIETY"
Babeş-Bolyai University, Cluj-Napoca, Romania.

Deutscher Akademischer Austausch Dienst (**DAAD**).

Stabilitätspakt für Südosteuropa gefördert durch Deutschland (**SOE**).